



Article

# P2Y<sub>2</sub> and P2X<sub>4</sub> Receptors Mediate Ca<sup>2+</sup> Mobilization in DH82 Canine Macrophage Cells

Reece Andrew Sophocleous <sup>1,2</sup> , Nicole Ashleigh Miles <sup>1,2</sup>, Lezanne Ooi <sup>1,2</sup> and Ronald Sluyter <sup>1,2,\*</sup>

<sup>1</sup> Illawarra Health and Medical Research Institute, Wollongong, NSW 2522, Australia; rs256@uowmail.edu.au (R.A.S.); nam993@uowmail.edu.au (N.A.M.); lezanne@uow.edu.au (L.O.)

<sup>2</sup> Molecular Horizons and School of Chemistry and Molecular Bioscience, University of Wollongong, Wollongong, NSW 2522, Australia

\* Correspondence: rsluyter@uow.edu.au; Tel.: +612-4221-5508

Received: 7 October 2020; Accepted: 12 November 2020; Published: 13 November 2020



**Abstract:** Purinergic receptors of the P2 subclass are commonly found in human and rodent macrophages where they can be activated by adenosine 5'-triphosphate (ATP) or uridine 5'-triphosphate (UTP) to mediate Ca<sup>2+</sup> mobilization, resulting in downstream signalling to promote inflammation and pain. However, little is understood regarding these receptors in canine macrophages. To establish a macrophage model of canine P2 receptor signalling, the expression of these receptors in the DH82 canine macrophage cell line was determined by reverse transcription polymerase chain reaction (RT-PCR) and immunocytochemistry. P2 receptor function in DH82 cells was pharmacologically characterised using nucleotide-induced measurements of Fura-2 AM-bound intracellular Ca<sup>2+</sup>. RT-PCR revealed predominant expression of P2X<sub>4</sub> receptors, while immunocytochemistry confirmed predominant expression of P2Y<sub>2</sub> receptors, with low levels of P2X<sub>4</sub> receptor expression. ATP and UTP induced robust Ca<sup>2+</sup> responses in the absence or presence of extracellular Ca<sup>2+</sup>. ATP-induced responses were only partially inhibited by the P2X<sub>4</sub> receptor antagonists, 2',3'-O-(2,4,6-trinitrophenyl)-ATP (TNP-ATP), paroxetine and 5-BDBD, but were strongly potentiated by ivermectin. UTP-induced responses were near completely inhibited by the P2Y<sub>2</sub> receptor antagonists, suramin and AR-C118925. P2Y<sub>2</sub> receptor-mediated Ca<sup>2+</sup> mobilization was inhibited by U-73122 and 2-aminoethoxydiphenyl borate (2-APB), indicating P2Y<sub>2</sub> receptor coupling to the phospholipase C and inositol triphosphate signal transduction pathway. Together this data demonstrates, for the first time, the expression of functional P2 receptors in DH82 canine macrophage cells and identifies a potential cell model for studying macrophage-mediated purinergic signalling in inflammation and pain in dogs.

**Keywords:** P2Y<sub>2</sub> receptor; P2X<sub>4</sub> receptor; canine; dog; purinergic signalling; DH82; macrophage; pain; neuroinflammation

## 1. Introduction

The activation of purinergic receptors by nucleotides such as adenosine 5'-triphosphate (ATP) and uridine 5'-triphosphate (UTP) is crucial for a number of inflammatory processes, including those in the central nervous system (CNS) such as chronic pain [1–4] and remyelination of nerves following injury to the CNS [5,6]. The P2 receptor family consists of seven mammalian ionotropic P2X receptors (P2X<sub>1-7</sub>) and eight mammalian metabotropic P2Y receptors (P2Y<sub>1,2,4,6,11-14</sub>) that can modulate intracellular Ca<sup>2+</sup> concentrations through direct ion channel permeation or mobilization of intracellular Ca<sup>2+</sup> stores, respectively [7]. P2 receptors, such as the P2X<sub>4</sub> and P2Y<sub>2</sub> receptors, are commonly expressed on human and rodent macrophages and macrophage cell lines [8–14], and have demonstrated roles in signalling

pathways that control chronic pain and inflammation in humans or rodents [2,8,15–18]. Despite this, studies on purinergic signalling in canine macrophages are lacking.

The DH82 cell line is a canine macrophage cell line isolated from a 10 year old Golden Retriever with malignant histiocytosis [19]. This cell line has recently been demonstrated as a useful model of canine macrophage physiology, bearing similarities to an M0 macrophage subtype with demonstrated potential for polarisation to either M1 or M2a subtypes through cytokine stimulation [20]. Studies have demonstrated that DH82 cells express a number of macrophage markers, such as CD11c and CD18 [21], and can secrete tumour necrosis factor (TNF)- $\alpha$  and interleukin (IL)-6 similar to that observed in lipopolysaccharide (LPS)-stimulated canine monocytes [22]. Despite its use as an in vitro model of viral and protozoan infection [23–25], knowledge regarding purinergic signalling in DH82 cells is limited to a single report describing ATP- and adenosine-induced cytokine release [26]. Although this study did not investigate any purinergic receptor per se, DH82 cells represent a possible model to study endogenous P2 receptors in canine macrophages for a number of reasons. Firstly, the original study revealed that ATP could alter cytokine expression in LPS-stimulated DH82 cells [26]. Secondly, infection of DH82 cells with canine distemper virus modulates inflammatory signalling pathways [27] that are common to P2X receptor-mediated signalling [28]. Thirdly, despite few studies analysing the expression of P2 receptors in dogs, it has been demonstrated that canine monocytes express P2X7 receptors [29,30]. Lastly, human and rodent macrophage or myeloid cell lines, such as THP-1 and RAW264.7 cells, are well-established models for studying endogenous P2 receptors commonly expressed on human and rodent macrophages [31–38].

The current study aimed to establish a canine macrophage model of P2 receptor signalling. Through investigation of canine P2 receptor expression and functional characterisation of these receptors, this study has identified the P2Y<sub>2</sub> receptor and, to a lesser extent, the P2X<sub>4</sub> receptor, as the primary functional P2 receptors in DH82 cells, which are responsible for nucleotide-mediated Ca<sup>2+</sup> mobilization.

## 2. Results

### 2.1. DH82 Cells Express Abundant P2RX4 mRNA Compared to Other P2 Receptors

To establish a P2 receptor mRNA expression profile for DH82 cells, cDNA was amplified by RT-PCR using primer pairs (Table S1) designed to genes encoding canine P2X1-7 receptors and canine P2Y<sub>1,2,4,6,11-14</sub> receptors and amplicons were semi-quantitatively analysed by agarose gel electrophoresis and densitometry. P2X<sub>4</sub> receptor mRNA was most abundant in DH82 cells, with relative amounts comparable to glyceraldehyde 3-phosphate dehydrogenase (*GAPDH*; Figure 1) and  $\beta$ -actin (*ACTB*; data not shown). Other P2X receptor mRNAs, including P2X<sub>1</sub> and P2X<sub>7</sub> receptors were detected, but to a much lesser degree than the P2X<sub>4</sub> receptor (Figure 1). Additionally, mRNA from a number of P2Y receptor subtypes were also detected, including P2Y<sub>1</sub>, P2Y<sub>2</sub>, P2Y<sub>6</sub> and P2Y<sub>11</sub> receptors, however, as with P2X<sub>1</sub> and P2X<sub>7</sub> receptors, these were expressed at greatly reduced levels compared to the P2X<sub>4</sub> receptor (Figure 1).

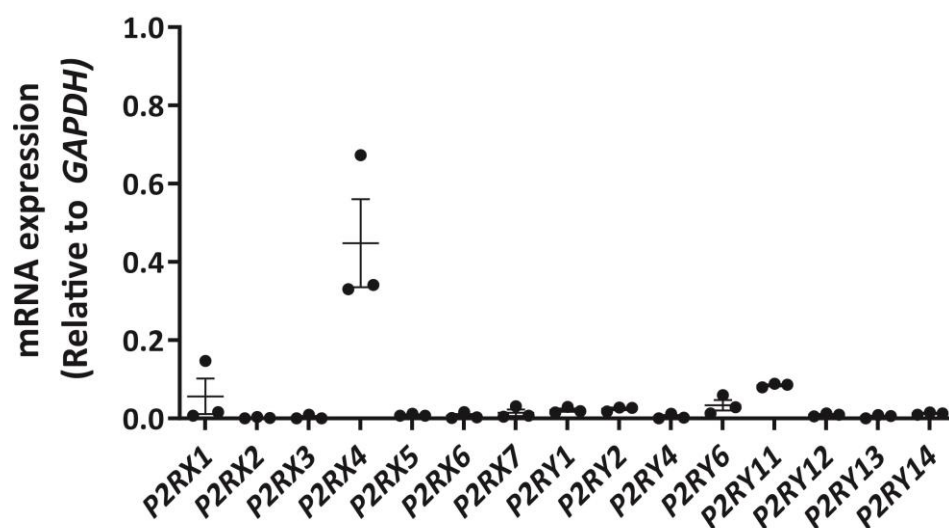


**Figure 1.** Expression of P2X and P2Y receptor mRNA in DH82 cells. RNA was isolated from DH82 cells and cDNA was synthesized and amplified using primer pairs designed to each respective *P2RX* or *P2RY* genes, with glyceraldehyde 3-phosphate dehydrogenase (*GAPDH*) as a positive control. Amplification in absence of cDNA was conducted for each primer pair to ensure primer specificity. Amplicons were visualized by agarose gel electrophoresis using GelRed and the GelDoc XR+ imaging system and semi-quantitatively analysed by densitometry. Data shown are the mean  $\pm$  SEM relative to *GAPDH* expression from three independent experiments.

## 2.2. Nucleotides Mediate $Ca^{2+}$ Responses in DH82 Cells

To establish an agonist profile for functional P2 receptors in DH82 cells, nucleotides which have previously demonstrated activity towards P2 receptors from dogs, humans or rodents [39,40] were utilised to measure changes in intracellular  $Ca^{2+}$ . These nucleotides were ATP, 3'-O-(4-benzoyl)benzoyl-ATP (BzATP), adenosine-5'-diphosphate (ADP), 2-methylthio-ADP (2MeSADP), uridine-5'-triphosphate (UTP) and uridine-5'-diphosphate (UDP). ADP was preincubated with hexokinase to remove trace amounts of ATP [41]. Incubation with ATP or UTP induced robust  $Ca^{2+}$  responses ( $\Delta F_{340/380}$ ) in DH82 cells, which peaked approximately 15 s after application of nucleotides (Figure 2A,B).  $Ca^{2+}$  responses then decayed more slowly, returning to baseline approximately 70–80 s after the initial peak was observed (Figure 2A,B). Incubation with ADP or BzATP resulted in much smaller  $Ca^{2+}$  responses compared to ATP and UTP (Figure 2C,D). UDP and 2MeSADP were unable to induce  $Ca^{2+}$  responses up to 30  $\mu$ M and 100  $\mu$ M, respectively (Figure 2E,F). Decay time, calculated as the time constant ( $\tau$ ), was similar for ATP and UTP ( $\tau = 56.9 \pm 4.8$  s and  $56.7 \pm 5.9$  s, respectively), however, BzATP ( $\tau = 102.3 \pm 17.9$  s) had a significantly longer decay time compared to ATP ( $p < 0.05$ ), UTP ( $p < 0.05$ ) or ADP ( $\tau = 23.8 \pm 0.4$  s;  $p < 0.001$ ), while UDP and 2MeSADP did not respond and as such, decay time could not be calculated (Figure 2G).

As  $Ca^{2+}$  responses were observed with a number of nucleotides, including those known to activate mammalian ionotropic P2X (ATP, BzATP) and metabotropic P2Y receptors (ATP, UTP, ADP), both the peak nucleotide-induced  $Ca^{2+}$  responses (Figure 2H) and net  $Ca^{2+}$  movement (Figure 2I; calculated as area under the curve [AUC]) were used for constructing concentration-response curves to account for potential differences in  $Ca^{2+}$  response phenotypes in a model of co-expression of P2X and P2Y receptor subtypes. In DH82 cells, nucleotides induced concentration-dependent  $Ca^{2+}$  responses with the rank order of potency of UTP > ATP  $\gg$  ADP  $\approx$  BzATP, with UDP and 2MeSADP being unresponsive (Figure 2H,I; Table 1). There were no significant differences between the  $EC_{50}$  values calculated for net  $Ca^{2+}$  movement and peak  $Ca^{2+}$  response for any nucleotide (Table 1).

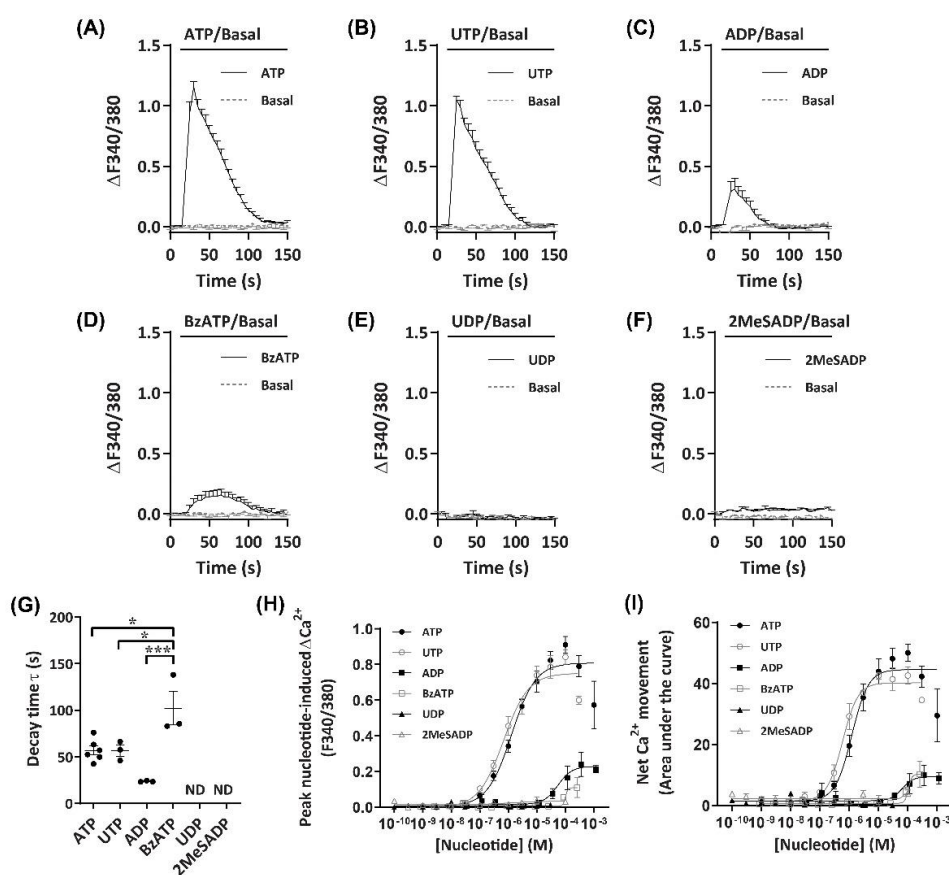


**Figure 2.** Nucleotide-induced  $\text{Ca}^{2+}$  response profiles for DH82 cells. (A–I) DH82 cells in extracellular  $\text{Ca}^{2+}$  solution (ECS) were loaded with Fura-2, incubated in the absence (basal) or presence of each nucleotide (as indicated) and Fura-2 fluorescence was recorded.  $\text{Ca}^{2+}$  traces ( $\Delta\text{F}340/380$ ) for (A) 100  $\mu\text{M}$  adenosine 5'-triphosphate (ATP) ( $n = 6$ ), (B) 30  $\mu\text{M}$  uridine 5'-triphosphate (UTP) ( $n = 3$ ), (C) 100  $\mu\text{M}$  adenosine 5'-diphosphate (ADP) (preincubated with 4.5 U/mL hexokinase for 1 h at 37 °C) ( $n = 3$ ), (D) 300  $\mu\text{M}$  3'-O-(4-benzoyl)benzoyl-ATP (BzATP) ( $n = 3$ ), (E) 30  $\mu\text{M}$  uridine 5'-diphosphate (UDP) ( $n = 3$ ) and (F) 100  $\mu\text{M}$  2-methylthio-ADP (2MeSADP) ( $n = 3$ ). (G) One phase decay time ( $\tau$ ) calculated from the peak of each  $\text{Ca}^{2+}$  trace, ND = no data. (H) Peak nucleotide-induced  $\text{Ca}^{2+}$  responses and (I) net  $\text{Ca}^{2+}$  movement were fit to the Hill equation to produce concentration-response curves ( $n$  values correspond to respective individual traces above). (A–I) Data shown are the mean  $\pm$  SEM from three to six independent experiments as indicated. (G) \*  $p < 0.05$  and \*\*\*  $p < 0.001$  between nucleotides as indicated analysed using a one-way ANOVA with Bonferroni post hoc test.

**Table 1.** Nucleotide-induced changes in intracellular  $\text{Ca}^{2+}$  in DH82 cells as measured by half maximal effective concentration.

Nucleotide	Peak $\text{Ca}^{2+}$ Response		Net $\text{Ca}^{2+}$ Response	
	pEC <sub>50</sub>	Hill Coefficient	pEC <sub>50</sub>	Hill Coefficient
ATP	5.88 $\pm$ 0.05 (100%)	0.99	5.92 $\pm$ 0.09 (100%)	1.43
UTP	6.16 $\pm$ 0.09 (65.9%)	1.02	6.26 $\pm$ 0.12 (69.1%)	1.71
ADP <sup>1</sup>	4.03 $\pm$ 0.30 (26.4%) <sup>2</sup>	1.47	4.07 $\pm$ 0.21 (19.9%) <sup>2</sup>	1.00
BzATP	<4.00 (12.1%) <sup>3</sup>	2.26	<4.00 (20.5%) <sup>3</sup>	2.66
UDP	ND (<10%)	-	ND (<10%)	-
2MeSADP	ND (<10%)	-	ND (<10%)	-

Abbreviations: AUC, area under the curve; ND, not determined (pEC<sub>50</sub> not calculated due to lack of response). Values in parentheses indicate the percent of each maximum agonist response compared to 100  $\mu\text{M}$  ATP.<sup>1</sup> ADP in the presence of hexokinase to remove contaminating ATP.<sup>2</sup>  $p < 0.05$  compared to the respective pEC<sub>50</sub> of ATP and UTP (one-way ANOVA).<sup>3</sup>  $p < 0.01$  compared to the respective pEC<sub>50</sub> of ATP and UTP (one-way ANOVA).

### 2.3. P2X4 Receptors Mediate Minor Changes in Intracellular $\text{Ca}^{2+}$ in DH82 Cells

#### 2.3.1. TNP-ATP Partially Reduces ATP-Induced Net $\text{Ca}^{2+}$ Movement

To determine if the observed  $\text{Ca}^{2+}$  responses were mediated by P2X receptors, DH82 cells were preincubated with the non-selective P2X receptor antagonist, 2',3'-O-(2,4,6-trinitrophenyl)-ATP (TNP-ATP) [42], then exposed to ATP. Preincubation with 50  $\mu\text{M}$  TNP-ATP partially reduced  $\text{Ca}^{2+}$  responses mediated by 10  $\mu\text{M}$  ATP, but did not significantly inhibit  $\text{Ca}^{2+}$  responses evoked by 1  $\mu\text{M}$  or 100  $\mu\text{M}$  ATP (Figure 3A–C). This was supported by a significant reduction in net  $\text{Ca}^{2+}$  movement at 10  $\mu\text{M}$  ATP, but not at other ATP concentrations (Figure 3E). Despite this, no significant change in peak  $\text{Ca}^{2+}$  response or shift in decay time was observed (Figure 3D,F). Preincubation with TNP-ATP did not result in a significant shift in the peak  $\text{Ca}^{2+}$  response  $\text{EC}_{50}$  for ATP, compared to cells preincubated in the absence of TNP-ATP (Figure 3D;  $\text{pEC}_{50}$   $5.38 \pm 0.08$  vs.  $5.57 \pm 0.13$ , respectively;  $p = 0.133$  Student's *t*-test). In contrast, preincubation with TNP-ATP did result in a significant shift in the net  $\text{Ca}^{2+}$  movement  $\text{EC}_{50}$  compared to cells preincubated in absence of TNP-ATP (Figure 2E;  $\text{pEC}_{50}$   $5.04 \pm 0.14$  vs.  $5.69 \pm 0.13$ , respectively;  $p = 0.007$  Student's *t*-test).

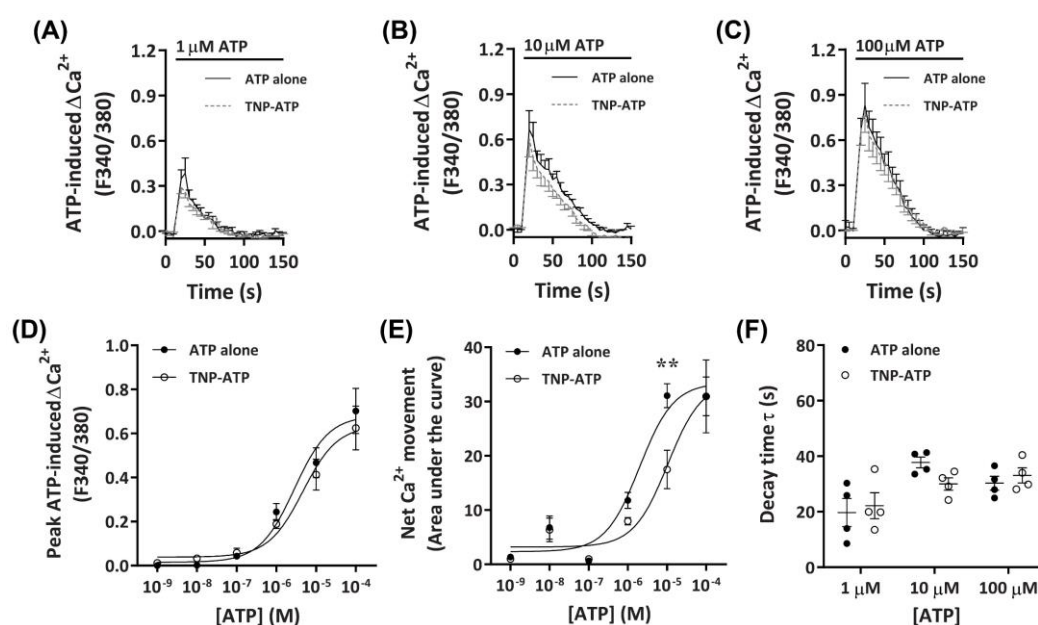


**Figure 3.** ATP-induced  $\text{Ca}^{2+}$  responses in DH82 cells in the absence or presence of 2',3'-O-(2,4,6-trinitrophenyl)-ATP (TNP-ATP). (A–F) DH82 cells in ECS were loaded with Fura-2 and preincubated in the absence (ATP alone) or presence of 50  $\mu\text{M}$  TNP-ATP (in ECS) for 5 min. Cells were exposed to increasing concentrations of ATP and Fura-2 fluorescence was recorded. (A–C) ATP-induced  $\text{Ca}^{2+}$  traces (F340/380) were plotted and the (D) peak  $\text{Ca}^{2+}$  response and (E) net  $\text{Ca}^{2+}$  movement were fit to the Hill equation to produce concentration-response curves. (F) One phase decay time ( $\tau$ ) calculated from the peak of each  $\text{Ca}^{2+}$  trace in (A–C). (A–F) Data shown are the mean  $\pm$  SEM from four independent experiments. (D–F)  $** p < 0.01$  compared to respective concentration of ATP alone analysed using a two-way ANOVA with Bonferroni post hoc test.

#### 2.3.2. Paroxetine Partially Reduces ATP-Induced Net $\text{Ca}^{2+}$ Movement

To further investigate the role of P2X receptors in DH82 cells, ATP-induced  $\text{Ca}^{2+}$  responses were measured in cells preincubated with paroxetine, a selective serotonin reuptake inhibitor which has been shown to inhibit P2X4 receptors [41,43,44] and human (but not rodent) P2X7 receptors [45,46]. Preincubation with paroxetine partially reduced  $\text{Ca}^{2+}$  responses mediated by ATP concentrations of 10  $\mu\text{M}$  or greater, with a small, but non-significant inhibitory effect observed at 1  $\mu\text{M}$  or below

(Figure 4A–C). Similar to TNP-ATP, preincubation with paroxetine did not significantly reduce peak  $\text{Ca}^{2+}$  responses (Figure 4D), however, did significantly reduce net  $\text{Ca}^{2+}$  movement and decay kinetics (Figure 4E,F). Preincubation with paroxetine did not significantly shift the  $\text{EC}_{50}$  of ATP compared to cells preincubated in absence of paroxetine for peak  $\text{Ca}^{2+}$  response (Figure 4D;  $\text{pEC}_{50}$   $5.55 \pm 0.31$  vs.  $5.51 \pm 0.48$ , respectively;  $p = 0.479$  Student's *t*-test) or net  $\text{Ca}^{2+}$  movement (Figure 4E;  $\text{pEC}_{50}$   $5.27 \pm 0.35$  vs.  $5.4 \pm 0.28$ , respectively;  $p = 0.387$  Student's *t*-test).

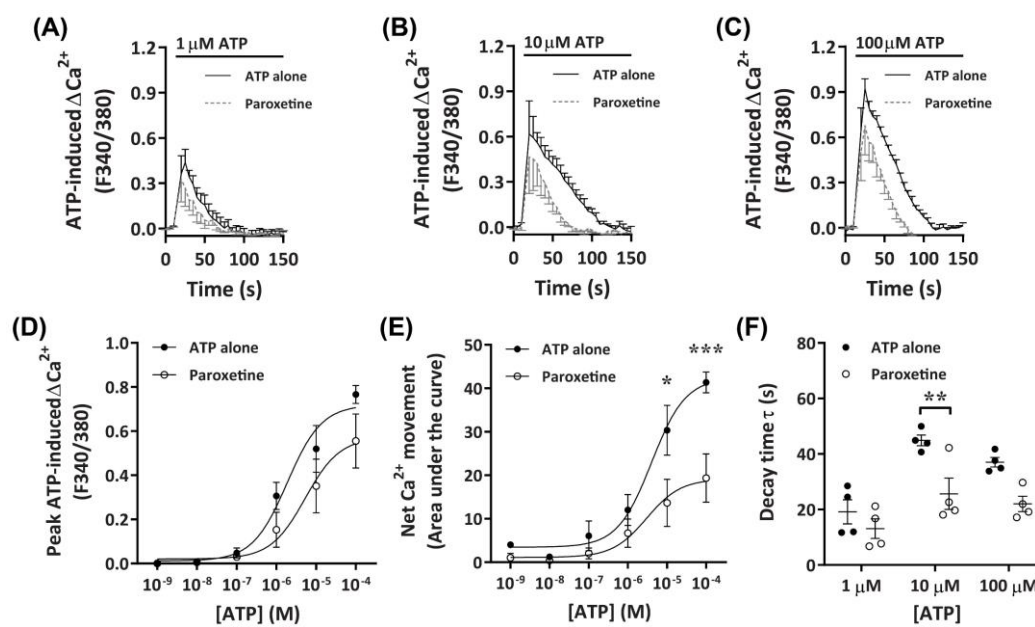


**Figure 4.** ATP-induced  $\text{Ca}^{2+}$  responses in DH82 cells in the absence or presence of paroxetine. (A–F) DH82 cells in ECS were loaded with Fura-2 and preincubated in the absence (ATP alone) or presence of 100  $\mu\text{M}$  paroxetine (both 0.3% dimethyl sulfoxide; DMSO) for 5 min. Cells were then exposed to increasing concentrations of ATP and Fura-2 fluorescence was recorded. (A–C) ATP-induced  $\text{Ca}^{2+}$  traces (F340/380) were plotted and the (D) peak  $\text{Ca}^{2+}$  response and (E) net  $\text{Ca}^{2+}$  movement were fit to the Hill equation to produce concentration-response curves. (F) One phase decay time ( $\tau$ ) calculated from the peak of each  $\text{Ca}^{2+}$  trace in (A–C). (A–F) Data shown are the mean  $\pm$  SEM from four independent experiments. (D–F) \*  $p < 0.05$ , \*\*  $p < 0.01$  and \*\*\*  $p < 0.001$  compared to respective concentration of ATP alone analysed using a two-way ANOVA with Bonferroni post hoc test.

### 2.3.3. 5-BDBD Partially Reduces ATP-Induced Net $\text{Ca}^{2+}$ Movement

To determine further if P2X4 receptors played a role in the observed ATP-induced  $\text{Ca}^{2+}$  responses, DH82 cells were preincubated with the selective P2X4 receptor antagonist, 5-BDBD, of which was recently demonstrated to inhibit the canine P2X4 receptor [41]. Preincubation with 30  $\mu\text{M}$  5-BDBD had no significant inhibitory effects on the  $\text{Ca}^{2+}$  response mediated by ATP (Figure 5A–C). There was no significant difference in the  $\text{EC}_{50}$  for cells preincubated in the absence or presence of 5-BDBD for ATP-induced peak  $\text{Ca}^{2+}$  response (Figure 5D;  $\text{pEC}_{50}$   $5.87 \pm 0.12$  vs.  $5.82 \pm 0.10$ , respectively;  $p = 0.372$  Student's *t*-test) or net  $\text{Ca}^{2+}$  movement (Figure 5E;  $\text{pEC}_{50}$   $5.73 \pm 0.18$  vs.  $5.64 \pm 0.14$ , respectively;  $p = 0.358$  Student's *t*-test), although a trend towards decreased net  $\text{Ca}^{2+}$  movement was observed at 10  $\mu\text{M}$  ATP (Figure 5E). Of note, there was a significant reduction in decay kinetics at 10  $\mu\text{M}$  ATP for cells preincubated in the presence of 5-BDBD compared to those in absence of the antagonist (Figure 5F).

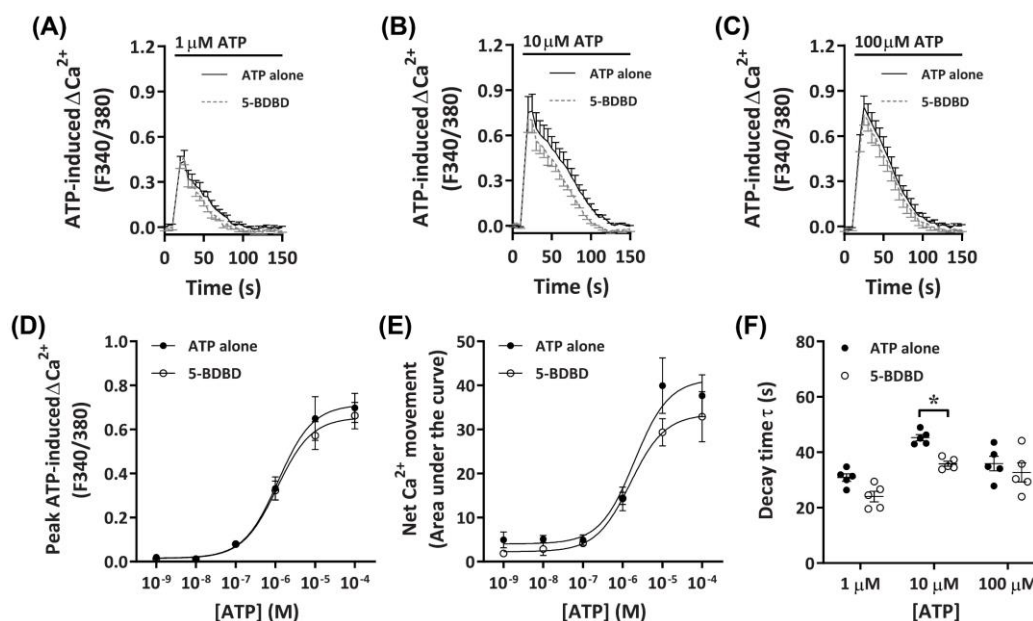


**Figure 5.** ATP-induced Ca<sup>2+</sup> responses in DH82 cells in the absence or presence of 5-BDBD. (A–F) DH82 cells in ECS were loaded with Fura-2 and preincubated in the absence (ATP alone) or presence of 30 μM 5-BDBD (both 0.3% DMSO) for 5 min. Cells were then exposed to increasing concentrations of ATP and Fura-2 fluorescence was recorded. (A–C) ATP-induced Ca<sup>2+</sup> traces (F340/380) were plotted and the (D) peak Ca<sup>2+</sup> response and (E) net Ca<sup>2+</sup> movement were fit to the Hill equation to produce concentration-response curves. (F) One phase decay time ( $\tau$ ) calculated from the peak of each Ca<sup>2+</sup> trace in (A–C). (A–F) Data shown are mean  $\pm$  SEM from five independent experiments. (D–F) \*  $p < 0.05$  compared to respective concentration of ATP alone analysed using a two-way ANOVA with Bonferroni post hoc test.

#### 2.3.4. Ivermectin Positively Modulates ATP-Induced Net Ca<sup>2+</sup> Movement

It has recently been demonstrated that ivermectin can effectively potentiate Ca<sup>2+</sup> responses mediated by canine P2X<sub>4</sub> receptors [41]. To further investigate if DH82 cells express functional P2X<sub>4</sub> receptors, cells were preincubated with ivermectin prior to activation with increasing concentrations of ATP. Preincubation with 3 μM ivermectin revealed a strong potentiation of ATP-induced Ca<sup>2+</sup> responses in DH82 cells (Figure 6A–C), with significant increases in ATP-induced net Ca<sup>2+</sup> movement and peak Ca<sup>2+</sup> response observed in the presence of ivermectin compared to cells preincubated in absence of ivermectin at ATP concentrations upwards of 10 μM (Figure 6D,E). Despite this, there was no significant difference in the EC<sub>50</sub> in the absence or presence of ivermectin for ATP-induced peak Ca<sup>2+</sup> response (Figure 6D; pEC<sub>50</sub> 5.76  $\pm$  0.19 vs. 5.37  $\pm$  0.35;  $p = 0.372$  Student's  $t$ -test) or net Ca<sup>2+</sup> movement (Figure 6E; pEC<sub>50</sub> 5.62  $\pm$  0.01 vs. 5.57  $\pm$  0.12, respectively;  $p = 0.358$  Student's  $t$ -test). Additionally, there were no significant differences in decay kinetics between cells preincubated in absence or presence of ivermectin (Figure 6F). Collectively this and the above data suggests that DH82 cells express functional P2X<sub>4</sub> receptors.

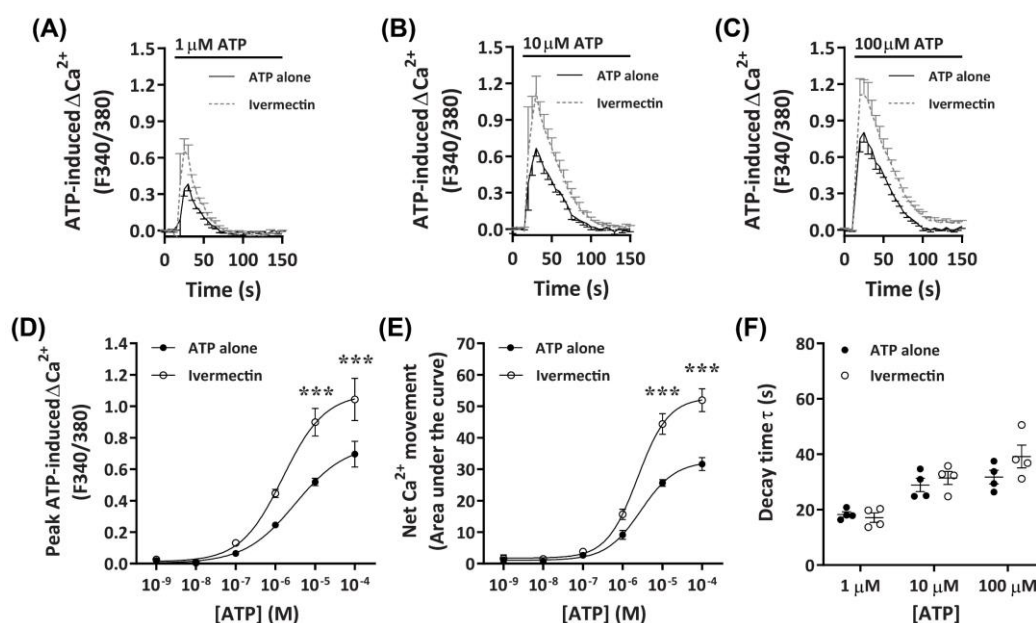


**Figure 6.** ATP-induced Ca<sup>2+</sup> responses in DH82 cells in the absence or presence of ivermectin. (A–F) DH82 cells in ECS were loaded with Fura-2 and preincubated in the absence (ATP alone) or presence of 3 μM ivermectin (both 0.1% DMSO) for 5 min. Cells were then exposed to increasing concentrations of ATP and Fura-2 fluorescence was recorded. (A–C) ATP-induced Ca<sup>2+</sup> traces (F340/380) were plotted and the (D) peak Ca<sup>2+</sup> response and (E) net Ca<sup>2+</sup> movement were fit to the Hill equation to produce concentration-response curves. (F) One phase decay time (τ) calculated from the peak of each Ca<sup>2+</sup> trace in (A–C). (A–F) Data shown are mean ± SEM from five independent experiments. (D–F) \*\*\* *p* < 0.001 compared to respective concentration of ATP alone analysed using a two-way ANOVA with Bonferroni post hoc test.

#### 2.4. ATP and UTP Mediate Both Ca<sup>2+</sup> Influx and Store-Operated Ca<sup>2+</sup> Entry in DH82 Cells

Despite the apparent P2X4-mediated effects on Ca<sup>2+</sup> responses in DH82 cells, a lack of complete inhibition by P2X receptor antagonists, as well as the responsiveness to UTP, suggest the presence of functional P2Y receptors in DH82 cells. To determine if G<sub>q/11</sub>-coupled P2Y receptors, which have demonstrated roles in store-operated Ca<sup>2+</sup> entry [47], were involved in the observed Ca<sup>2+</sup> responses in DH82 cells, nucleotide-induced changes in intracellular Ca<sup>2+</sup> were measured in the presence of extracellular or intracellular Ca<sup>2+</sup> chelators. Compared to cells in the presence of extracellular Ca<sup>2+</sup> (Figure 7A,F), cells incubated with ethylene glycol tetraacetic acid (EGTA) demonstrated a partial reduction in ATP- and UTP-induced Ca<sup>2+</sup> responses (Figure 7B,G). This was supported by significant reductions in decay time (Figure 7K) and net Ca<sup>2+</sup> movement (Figure 7L,M) for both ATP- and UTP-mediated responses. In contrast, preincubation with the cell-permeant Ca<sup>2+</sup> chelator, 1,2-bis(2-aminophenoxy)ethane-*N,N,N',N'*-tetraacetic acid tetrakis(acetoxymethyl ester) (BAPTA-AM), near completely reduced ATP- and UTP-induced Ca<sup>2+</sup> responses (Figure 7C,H) and net Ca<sup>2+</sup> movement (Figure 7L,M) in DH82 cells. Treatment with thapsigargin, to inhibit sarco/endoplasmic reticulum Ca<sup>2+</sup> ATPase pumps [48], near completely reduced ATP- and UTP-induced Ca<sup>2+</sup> responses in the presence of extracellular Ca<sup>2+</sup> (ECS; Figure 7D,I,L,M) and completely reduced these responses in the absence of extracellular Ca<sup>2+</sup> (EGTA; Figure 7E,J,L,M). Together, this suggests the involvement of both P2X and P2Y receptors in DH82 cells for mediating changes in intracellular Ca<sup>2+</sup> in response to activation by nucleotides.



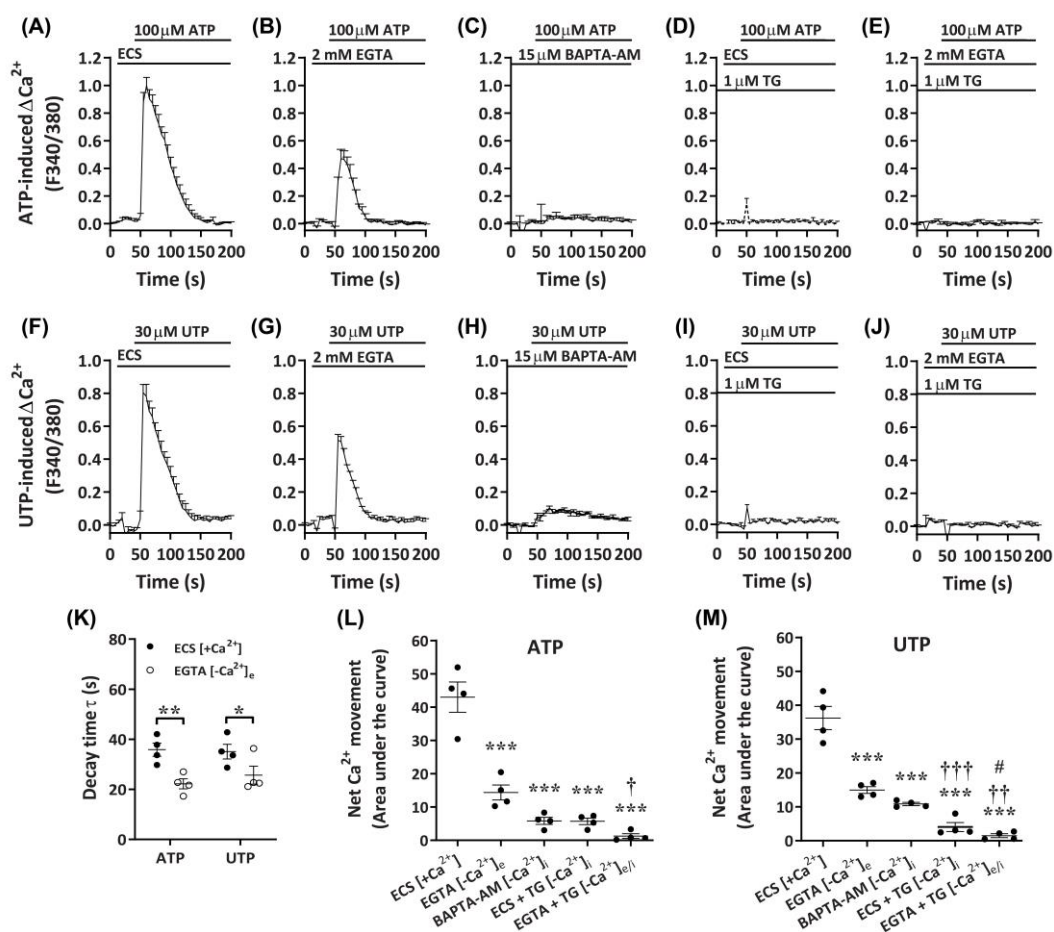


**Figure 7.** Nucleotide-induced  $Ca^{2+}$  responses in the absence or presence of extracellular and/or intracellular  $Ca^{2+}$ . (A–M) DH82 cells in (A,D,F,I) ECS or (B,C,E,G,H,J)  $Ca^{2+}$ -free solution were loaded with Fura-2 and preincubated in the absence (A,D,F,I) (ECS) or presence (B,E,F,J) of 2 mM ethylene glycol tetraacetic acid EGTA for 30 s, (C,H) 15  $\mu M$  1,2-bis(2-aminophenoxy)ethane-*N,N,N',N'*-tetraacetic acid tetrakis(acetoxymethyl ester) (BAPTA-AM) for 30 min or (D,E,I,J) 1  $\mu M$  thapsigargin (TG) for 30 min prior to incubation in the absence (D,I) or presence (E,J) of 2 mM EGTA. (A–M) Cells were then exposed to (A–E) 100  $\mu M$  ATP or (F–J) 30  $\mu M$  UTP and Fura-2 fluorescence was recorded. (K) One phase decay time ( $\tau$ ) calculated from the peak of each  $Ca^{2+}$  trace in (A,B,F,G). (L,M) Net  $Ca^{2+}$  movement from each trace in A–J. (A–M) Data shown are the mean  $\pm$  SEM from four independent experiments. \*  $p < 0.05$ , \*\*  $p < 0.01$  and \*\*\*  $p < 0.001$  compared to respective ECS alone control; †  $p < 0.05$ , ††  $p < 0.01$  and †††  $p < 0.001$  compared to EGTA; #  $p < 0.05$  compared to BAPTA-AM analysed using a (K) Student's *t*-test or (L,M) one-way ANOVA with Bonferroni post hoc test.

## 2.5. P2Y<sub>2</sub> Receptor Activation Mediates $Ca^{2+}$ Mobilization in DH82 Cells

### 2.5.1. Suramin Reduces ATP- and UTP-Induced $Ca^{2+}$ Mobilization

The data presented above suggests a major role for an ATP- and UTP-responsive P2Y receptor in  $Ca^{2+}$  mobilization within DH82 cells. Previous studies have demonstrated that the canine P2Y<sub>2</sub> receptor in Madin–Darby canine kidney (MDCK) cells responds to both ATP and UTP with similar potency [49]. Therefore, to determine if nucleotide-induced  $Ca^{2+}$  mobilization was mediated by P2Y<sub>2</sub> receptors, DH82 cells were preincubated with increasing concentrations of the non-selective P2 receptor antagonist, suramin [50], which is selective for P2Y<sub>2</sub> over P2Y<sub>4</sub> receptors [51]. Cells were then incubated with ATP or UTP at their respective EC<sub>80</sub> to determine the optimal concentration for P2Y receptor inhibition. Preincubation of DH82 cells with 1 mM suramin inhibited  $Ca^{2+}$  responses evoked

by 3  $\mu\text{M}$  ATP, however lower concentrations of suramin (<100  $\mu\text{M}$ ) had little to no inhibitory effect (Figure 8A). In contrast, preincubation with 100  $\mu\text{M}$  and 1 mM, but not 10  $\mu\text{M}$  suramin or less inhibited  $\text{Ca}^{2+}$  responses evoked by 1  $\mu\text{M}$  UTP (Figure 8B). Inhibitory effects observed in the presence of 100  $\mu\text{M}$  suramin resulted in significant shifts in the  $\text{IC}_{50}$  of suramin between ATP- and UTP-induced peak  $\text{Ca}^{2+}$  responses (Figure 8C;  $\text{pIC}_{50}$   $3.02 \pm 0.06$  and  $3.70 \pm 0.05$ , respectively;  $p < 0.001$  Student's *t*-test) and net  $\text{Ca}^{2+}$  movement (Figure 8D;  $\text{pIC}_{50}$   $3.03 \pm 0.12$  and  $3.54 \pm 0.14$ , respectively;  $p = 0.025$  Student's *t*-test).

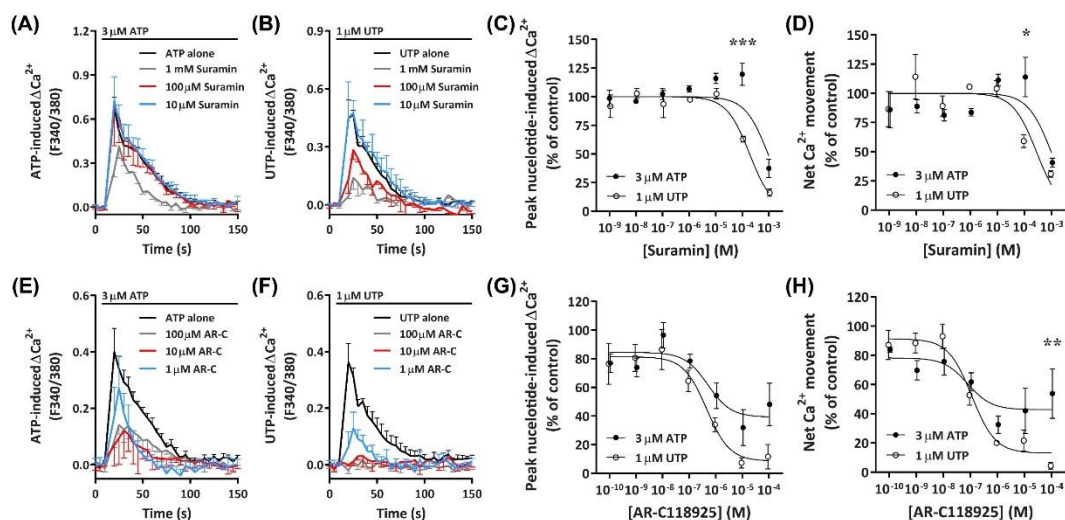


**Figure 8.** ATP- and UTP-induced  $\text{Ca}^{2+}$  responses in DH82 cells in the absence or presence of suramin or AR-C118925. (A–H) DH82 cells in ECS were loaded with Fura-2 and preincubated in the absence or presence of increasing concentrations of (A–D) suramin (in ECS) or (E–H) AR-C118925 (AR-C; 0.3% DMSO) for 30 min. Cells were then exposed to 3  $\mu\text{M}$  ATP or 1  $\mu\text{M}$  UTP (respective  $\text{EC}_{80}$  values) and Fura-2 fluorescence was recorded. Nucleotide-induced (C,G) peak  $\text{Ca}^{2+}$  response and (D,H) net  $\text{Ca}^{2+}$  movement were normalised to 3  $\mu\text{M}$  ATP or 1  $\mu\text{M}$  UTP alone and expressed as a percentage of the response in absence of inhibitor (% of control). Data were then fit to the Hill equation to produce concentration-response curves and calculate the  $\text{IC}_{50}$ . (A–H) Data shown are mean  $\pm$  SEM from three independent experiments. \*  $p < 0.05$ , \*\*  $p < 0.01$  and \*\*\*  $p < 0.001$  compared to respective concentration of antagonist with ATP or UTP analysed using a two-way ANOVA with Bonferroni post hoc test.

### 2.5.2. AR-C118925 Reduces ATP- and UTP-Induced $\text{Ca}^{2+}$ Mobilization

To determine if the  $\text{P2Y}_2$  receptor was mediating nucleotide-induced  $\text{Ca}^{2+}$  mobilization in DH82 cells, the selective  $\text{P2Y}_2$  receptor antagonist AR-C118925 [52] was preincubated with cells prior to incubation with ATP or UTP at their respective  $\text{EC}_{80}$  concentrations. AR-C118925 at concentrations of 1  $\mu\text{M}$  or greater could only partially inhibit  $\text{Ca}^{2+}$  responses evoked by 3  $\mu\text{M}$  ATP (Figure 8E). In contrast, preincubation with AR-C118925 at concentrations of 10  $\mu\text{M}$  or greater near completely inhibited  $\text{Ca}^{2+}$  responses evoked by 1  $\mu\text{M}$  UTP (Figure 8F). A significant shift was observed in the  $\text{IC}_{50}$  of AR-C118925 in response to activation by ATP and UTP calculated using peak  $\text{Ca}^{2+}$  responses (Figure 8G;  $\text{pIC}_{50}$   $6.18 \pm 0.16$  and  $6.61 \pm 0.09$ , respectively;  $p = 0.033$  Student's *t*-test), but not net  $\text{Ca}^{2+}$  movement (Figure 8H;  $\text{pIC}_{50}$   $6.67 \pm 0.19$  and  $6.87 \pm 0.12$ , respectively;  $p = 0.198$  Student's *t*-test). The inhibition of nucleotide-induced  $\text{Ca}^{2+}$  responses by AR-C118925 supports the presence of  $\text{P2Y}_2$  receptors in DH82 cells. Moreover, the differing effect of this antagonist on ATP- and UTP-induced responses indicates the presence of other  $\text{P2}$  receptors in this cell line. Additionally, preincubation of DH82 cells together with 5-BDBD and AR-C118925 resulted in a complete inhibition of both ATP- and UTP-induced net  $\text{Ca}^{2+}$  movement (Figure S1), further suggesting a role for both  $\text{P2X}_4$  and  $\text{P2Y}_2$  receptors in nucleotide-mediated  $\text{Ca}^{2+}$  responses in DH82 cells.

### 2.6. DH82 Canine Macrophages Predominantly Express Cell Surface P2Y<sub>2</sub> Receptors

To confirm the presence of P2X<sub>4</sub> and P2Y<sub>2</sub> receptors, DH82 cells were analysed by immunocytochemistry and confocal microscopy using anti-P2X<sub>4</sub> or anti-P2Y<sub>2</sub> receptor antibodies. Confocal microscopy revealed the presence of both P2X<sub>4</sub> and P2Y<sub>2</sub> receptors in fixed and permeabilised DH82 cells (Figure 9A,B). The expression of P2X<sub>4</sub> receptors was relatively low and largely intracellular (Figure 9A). The expression of P2Y<sub>2</sub> receptors on DH82 cells was considerably higher and predominantly localised to the cell surface (Figure 9B), consistent with its reported expression in the membrane of MDCK cells [53,54]. No fluorescence was detected in DH82 cells stained with secondary antibodies alone (Figure S2).

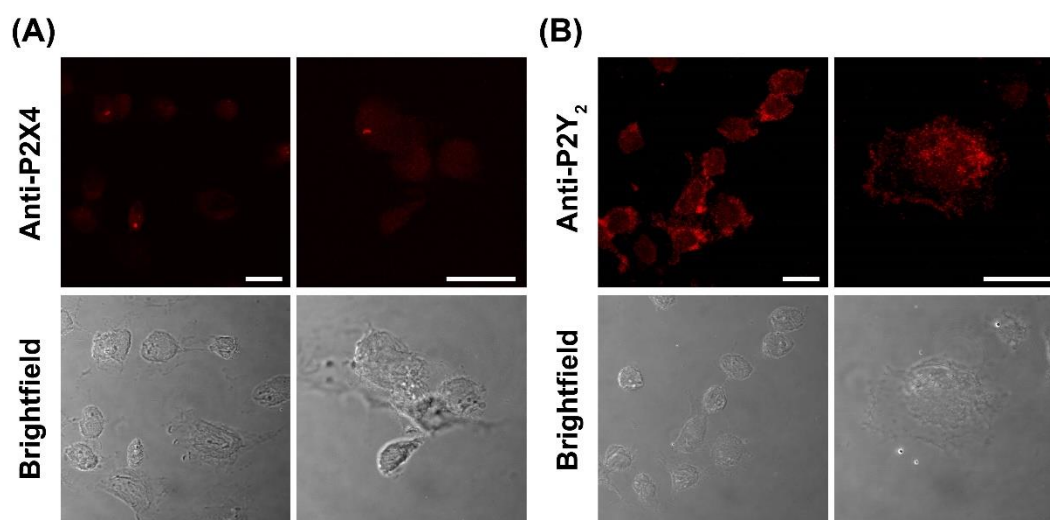


**Figure 9.** Expression of P2X<sub>4</sub> and P2Y<sub>2</sub> receptors in DH82 cells. DH82 cells were fixed, permeabilized and labelled with (A) anti-P2X<sub>4</sub> or (B) anti-P2Y<sub>2</sub> receptor primary antibodies, then with anti-goat<sup>594</sup> or anti-rabbit<sup>594</sup> secondary antibodies, respectively. Cells were imaged by confocal microscopy. Scale bar = 20  $\mu$ m. Results are representative of three independent experiments.

### 2.7. P2Y<sub>2</sub> Receptor Activation Downstream Ca<sup>2+</sup> Mobilization Is Coupled to the Phospholipase C/Inositol Triphosphate Signal Transduction Pathway in DH82 Cells

Functional P2Y<sub>2</sub> receptors have been reported in human and rodent macrophages [9,10], where they can activate phospholipase C (PLC) and inositol trisphosphate (IP<sub>3</sub>) receptors, leading to Ca<sup>2+</sup> mobilization from endoplasmic reticulum stores [8,12]. To determine if activation of canine P2Y<sub>2</sub> receptors in DH82 macrophage cells results in a similar downstream signalling pathway, cells were preincubated with antagonists of PLC (U-73122) and IP<sub>3</sub> receptors (2-aminoethoxydiphenyl borate; 2-APB), and nucleotide-induced intracellular Ca<sup>2+</sup> mobilization was recorded in absence of extracellular Ca<sup>2+</sup>. The presence of AR-C118925 under these conditions was also examined. Preincubation of DH82 cells with AR-C118925 near completely inhibited intracellular Ca<sup>2+</sup> mobilization mediated by ATP (Figure 10A; 90.5  $\pm$  3.3% inhibition) or UTP (Figure 10B; 87.3  $\pm$  7.4% inhibition). Similarly, preincubation of DH82 cells with 75  $\mu$ M 2-APB near completely inhibited intracellular Ca<sup>2+</sup> mobilization mediated by ATP (Figure 10A; 90.7  $\pm$  4.4% inhibition) or UTP (Figure 10B; 91.2  $\pm$  3.1% inhibition). In contrast, preincubation with 5  $\mu$ M U-73122 only partially reduced intracellular Ca<sup>2+</sup> mobilization mediated by ATP (Figure 10A; 64.9  $\pm$  5.9% inhibition) or UTP (Figure 10B; 55.5  $\pm$  8.7% inhibition). The combination of two or three of these antagonists completely impaired ATP- and UTP-induced Ca<sup>2+</sup> responses (Figure 10A,B). Thus, preincubation with AR-C118925, 2-APB, U-73122 or any combination of these antagonists resulted in a significant reduction of intracellular Ca<sup>2+</sup> mobilization ( $p < 0.001$ , one-way ANOVA) compared to that mediated by ATP (Figure 10A) or UTP (Figure 10B) in the absence of antagonists.

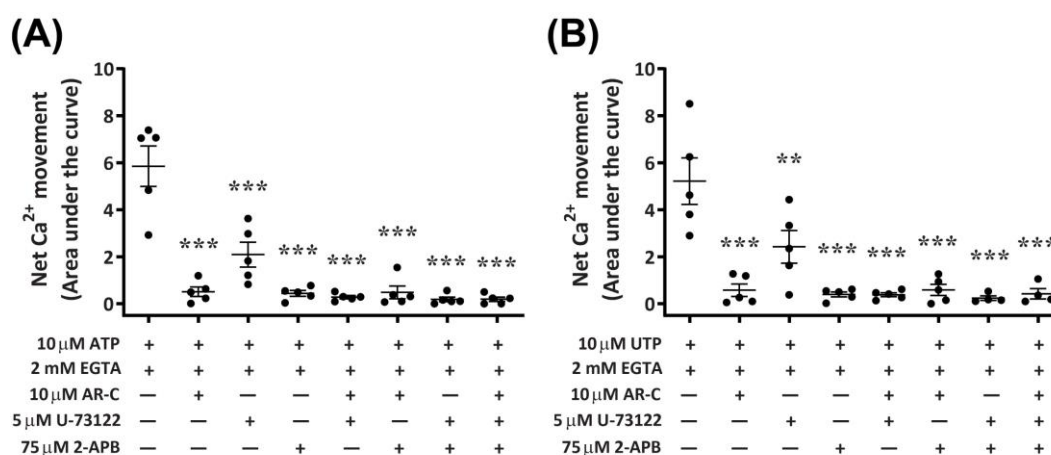


**Figure 10.** Nucleotide-induced  $\text{Ca}^{2+}$  mobilization in DH82 cells depleted of extracellular  $\text{Ca}^{2+}$  in the absence or presence of AR-C118925, U-73122 and 2-APB. DH82 cells were loaded with Fura-2 and preincubated in  $\text{Ca}^{2+}$ -free solution containing 2 mM EGTA in the absence or presence of 10  $\mu\text{M}$  AR-C118925 (AR-C; 0.03% DMSO), 5  $\mu\text{M}$  U-73122 (0.05% DMSO) or 75  $\mu\text{M}$  2-APB (0.15% DMSO) for 5 min. Cells were then exposed to (A) 10  $\mu\text{M}$  ATP or (B) 10  $\mu\text{M}$  UTP and Fura-2 fluorescence was recorded. Data shown are the mean  $\pm$  SEM from five independent experiments. \*\*  $p < 0.01$  and \*\*\*  $p < 0.001$  compared to respective nucleotide alone, analysed using a one-way ANOVA with Bonferroni post hoc test.

### 3. Discussion

To date, the DH82 canine macrophage cell line has primarily been utilized as a model of viral and protozoan infection [23–25], such as for the study of canine distemper and its oncolytic potential [55–57]. Although studies have described the expression of functional P2 receptors in human or rodent macrophages and macrophage cell lines [8,10,11,34], studies directly investigating P2 receptors in canine macrophages have been absent. The current study described, for the first time, the expression and function of P2 receptors in DH82 cells, demonstrating a primary role for cell surface  $\text{P2Y}_2$  receptors in nucleotide-mediated  $\text{Ca}^{2+}$  mobilization through PLC/ $\text{IP}_3$  signal transduction. This study also demonstrates a minor functional role for  $\text{P2X}_4$  receptors in DH82 cells, suggesting this cell line may present as a suitable model for studying P2 receptor-mediated inflammation and pain signalling in dogs.

The agonist profile of ATP on DH82 cells demonstrated pharmacological similarities to the recombinant canine  $\text{P2X}_4$  receptor [41], as well as studies of endogenous  $\text{P2X}_4$  receptors in a human macrophage cell model [34]. BzATP induced partial  $\text{Ca}^{2+}$  responses in DH82 cells with significantly lower potency compared to ATP, consistent with the recent report that BzATP is a partial agonist of recombinant canine  $\text{P2X}_4$  receptors [41]. In addition, the increased decay kinetics of  $\text{Ca}^{2+}$  responses evoked by BzATP, compared to ATP, further supports a role for  $\text{P2X}_4$  receptors in the observed  $\text{Ca}^{2+}$  responses [41]. TNP-ATP and paroxetine, two non-selective antagonists of  $\text{P2X}_4$  receptors [44], as well as 5-BDBD, a selective  $\text{P2X}_4$  receptor antagonist [58], had minor inhibitory effects on ATP-induced  $\text{Ca}^{2+}$  responses in DH82 cells. Although it has recently been demonstrated that these antagonists can inhibit recombinant canine  $\text{P2X}_4$  receptors, the minor inhibition observed with these antagonists in DH82 cells were potentially in part due a lack of potency towards the canine  $\text{P2X}_4$  receptor [41], as well as the relatively low expression of  $\text{P2X}_4$  receptors in DH82 cells observed by immunocytochemistry. In contrast, ivermectin, the positive allosteric modulator which is routinely used to investigate  $\text{P2X}_4$  receptor activity [59], demonstrated strong potentiation of ATP-induced  $\text{Ca}^{2+}$  responses and efficacy of ATP, with little effect on decay time. This data further supports the expression of functional  $\text{P2X}_4$  receptors in canine macrophages, however, it suggests that potentiation or upregulation of  $\text{P2X}_4$  receptors may first be required to observe notable responses.

Consistent with the pharmacological profiles reported for the canine P2Y<sub>2</sub> receptor cloned from MDCK cells [49], both ATP and UTP induced robust Ca<sup>2+</sup> responses in DH82 cells with similar EC<sub>50</sub> values. These responses were observed even in the absence of extracellular Ca<sup>2+</sup>, consistent with the P2Y-mediated mobilization of intracellular Ca<sup>2+</sup> [60]. Similar to the current study with DH82 cells, other studies have also demonstrated that ADP is a low-potency agonist of the canine P2Y<sub>2</sub> receptor cloned from MDCK cells [49,61]. In addition, incubation of DH82 cells with BzATP revealed pharmacological similarities to that observed with human P2Y<sub>2</sub> receptors, where BzATP is ineffective at concentrations below 100 μM [33,62]. Collectively, this suggests that functional P2Y<sub>2</sub> receptors were responsible for nucleotide-induced Ca<sup>2+</sup> mobilization in DH82 cells. This was supported by inhibition observed in the presence of the P2Y<sub>2</sub> receptor antagonists, suramin and AR-C118925. Despite suramin lacking potency and selectivity, it remains a valuable tool in characterising P2Y receptor responses, as it is considered a low-potency antagonist of P2Y<sub>2</sub> receptors, but is relatively insensitive to P2Y<sub>4</sub> receptors [51,63]. This suggests that the ATP/UTP-sensitive P2Y<sub>2</sub>, but not P2Y<sub>4</sub> receptor, is responsible for the observed Ca<sup>2+</sup> mobilization, consistent with the expression of P2Y<sub>2</sub> receptors in DH82 cells determined by confocal microscopy. Notably, P2Y<sub>2</sub> receptor protein expression was greater than that of P2X<sub>4</sub> receptor protein expression, with an opposite pattern observed for mRNA expression of these receptors. Reasons for this discrepancy remain unknown, but a lack of correlation between mRNA and protein expression is well documented and attributed to various contributing factors related to post-transcriptional and post-translational regulation of mRNA and protein expression [64].

A number of other canine P2Y receptors from MDCK cells have been cloned and characterised, including the P2Y<sub>1</sub> and P2Y<sub>11</sub> receptors [49,65,66], of which mRNA of both these receptors were detected in DH82 cells. The nucleotide agonist profile of canine P2Y<sub>11</sub> receptors differs markedly from the human P2Y<sub>11</sub> receptor, where ATP is a potent agonist of human, but not canine P2Y<sub>11</sub> receptors, and ADP and its analogue 2MeSADP are potent agonists of canine, but not human P2Y<sub>11</sub> receptors [66]. In the current study, it was revealed that ATP, but not ADP, was a moderately potent mediator of Ca<sup>2+</sup> responses in DH82 cells, while no such responses were observed with 2MeSADP. BzATP is also a full agonist of human P2Y<sub>11</sub> receptors [67], further suggesting that DH82 cells likely do not express functional P2Y<sub>11</sub> receptors. ADP and 2MeSADP have also been reported as potent agonists of the canine P2Y<sub>1</sub> receptor [68]. However, it was demonstrated in the current study that only ADP, but not 2MeSADP, induced a small Ca<sup>2+</sup> response in DH82 cells. Although this could suggest that DH82 cells express low amounts of functional P2Y<sub>1</sub> receptors, the complete lack of response to 2MeSADP suggests that P2Y<sub>1</sub> receptors are unlikely to be responsible for P2Y receptor-mediated Ca<sup>2+</sup> mobilisation in DH82 cells. Additionally, a complete lack of Ca<sup>2+</sup> response in DH82 cells incubated with the P2Y<sub>6</sub> receptor agonist, UDP [69,70], strongly suggests that DH82 cells do not express functional P2Y<sub>6</sub> receptors.

The current study demonstrated that nucleotide-mediated Ca<sup>2+</sup> mobilization in DH82 cells was also inhibited by antagonists of PLC and IP<sub>3</sub> receptors, U-73122 and 2-APB, respectively. This was consistent with previous studies that demonstrate coupling of P2Y<sub>2</sub> receptors to G<sub>q/11</sub> and downstream signalling pathways in MDCK cells [49,65,71]. While 2-APB near completely inhibited Ca<sup>2+</sup> mobilisation, U-73122 only resulted in partial inhibition, although higher concentrations (>10 μM) have been shown to completely block P2Y<sub>2</sub> receptor-mediated Ca<sup>2+</sup> responses [72]. Notably, pre-incubation with P2Y<sub>2</sub> receptor antagonists resulted in approximately two-fold greater inhibition of UTP-induced Ca<sup>2+</sup> responses compared to ATP-induced responses, suggesting that ATP remained active at other receptors involved in mediating changes in intracellular Ca<sup>2+</sup>, such as P2X<sub>4</sub> receptors, which are also relatively insensitive to suramin [73]. In addition, both ATP- and UTP-induced Ca<sup>2+</sup> responses could be completely inhibited by co-incubation with 5-BDBD and AR-C118925, supporting a role for both P2X<sub>4</sub> and P2Y<sub>2</sub> receptors in DH82 cells.

Pro-monocytic and macrophage-like cell lines, such as human THP-1 cells, have recently proven useful models for studying endogenous purinergic signalling via P2X<sub>4</sub> and P2Y<sub>2</sub> receptors [10,13,34]. However, studies have demonstrated that these cell lines can be polarised towards a more specialised macrophage phenotype, in which the expression of P2 receptors, such as P2X<sub>4</sub> and P2X<sub>7</sub> receptors,

are commonly upregulated [34,38,74]. A study has recently demonstrated that DH82 canine macrophage cells could be polarised towards the M1 or M2a subtype through cytokine stimulation [20]. However, the DH82 cells utilised throughout this study remained unpolarised (M0) and, thus, it remains to be determined if cytokine stimulation influences P2 receptor expression or function. To this end, future studies could determine the purinergic signalling landscape of polarised DH82 cells. Future studies could also analyse P2 receptor expression and signalling in native canine macrophages. Given the known expression of P2X7 receptors on canine monocytes [29,30], canine monocyte-derived macrophages may provide a suitable candidate for the study of other purinergic receptors in native canine macrophages.

The upregulation of P2X4 receptors in macrophages and microglia has been highlighted as a key component in the signalling of inflammatory conditions, including chronic inflammatory and neuropathic pain [75,76], and remyelination of damaged nerves in the CNS [77]. P2X4 receptors, which reside primarily within lysosomes of macrophages, can be upregulated at the cell surface through lysosomal exocytosis [78]. This process plays a key role in  $\text{Ca}^{2+}$  homeostasis, ATP release and local activation of cell surface purinergic receptors [79]. Notably, activation of the C-C chemokine receptor 2 (CCR2) by C-C chemokine ligand 2 (CCL2) is known to mediate lysosomal exocytosis [80], while in rat alveolar macrophages and human THP-1 cells it has been demonstrated that the activation of cell surface P2Y<sub>2</sub> receptors induces the upregulation and secretion of CCL2 [8,10]. Thus, it could be suggested that activation of macrophage P2Y<sub>2</sub> receptors results in a P2 receptor signalling feedback mechanism which results in an increase in  $\text{Ca}^{2+}$  flux through upregulation of lysosomal exocytosis and trafficking of P2X4 receptors to the cell surface, leading to the release of prostaglandin E<sub>2</sub> and subsequent chronic inflammatory pain signalling [2]. These activated macrophages may also modulate microglial P2X4 receptors to control neuroinflammatory signalling following injury to the central nervous system [81]. Given the expression profile of these receptors in DH82 canine macrophages, this cell line may provide a suitable model for studying inflammatory pain signalling mechanisms of dogs in vitro, as well as for the pre-clinical testing of novel therapeutics targeting chronic pain.

Finally, although the sequence of P2X4 and P2Y<sub>2</sub> receptors in DH82 cells is yet to be determined, it remains of interest to identify novel single nucleotide polymorphisms should they exist in the genes encoding these receptors in dogs. A recent whole genome study of 582 dogs has revealed at least one missense variant (Ala9Asp) within the canine *P2RX4* gene and two missense variants (Gly193Ser and Val375Ile) within the canine *P2RY2* gene [82] (data accessed from the European Variation Archive; <https://www.ebi.ac.uk/eva/>). Whilst the effects of single nucleotide polymorphisms in the canine *P2RX4* and *P2RY2* genes are largely unknown, it has been demonstrated that single nucleotide polymorphisms of the genes encoding the human P2X4 and P2Y<sub>2</sub> receptors can alter receptor function [83,84]. Notably, in human macrophages, a 312Ser polymorphism of the P2Y<sub>2</sub> receptor has been demonstrated to alter secretion of CCL<sub>2</sub> following activation by UTP [10], suggesting a potential association with macrophage-mediated chronic inflammatory pain signalling. Despite this however, studies by our group have demonstrated that the canine *P2RX4* and *P2RX7* genes are much more conserved than their human counterparts [41,85,86] and, as such, naturally-occurring polymorphisms in the canine *P2RY2* gene may also be rare or limited to uncommon breeds not frequently sampled in canine whole genome studies.

In conclusion, the current study demonstrates for the first time, that DH82 canine macrophages primarily express functional P2Y<sub>2</sub> receptors and low levels of functional P2X4 receptors. As such, DH82 cells provide the first canine macrophage cell line for the study of endogenous P2X4 and P2Y<sub>2</sub> receptors. The data presented here provides indirect evidence that P2X4 and P2Y<sub>2</sub> receptors play a role in mediating changes in intracellular  $\text{Ca}^{2+}$  in canine macrophages in vivo. This mimics events observed in human and rodent macrophages and macrophage cell lines, where these P2 receptors have been suggested to play a key role in inflammation and chronic pain. Thus, DH82 cells may aid in the study of P2 receptor-mediated inflammation, including neuroinflammatory signalling processes, as well as preclinical screening of novel P2 receptor-targeting compounds for potential use in the treatment of inflammatory conditions, such as chronic pain in dogs.

## 4. Materials and Methods

### 4.1. Compounds and Reagents

BSA, EGTA and reagents for producing  $\text{Ca}^{2+}$  solutions were from Amresco (Solon, OH, USA). Fetal bovine serum (FBS) was purchased from Bovogen Biologicals (East Keilor, Melbourne, Australia) and heat inactivated at 56 °C for 30 min before use. 2-APB, U-73122 and UDP were from Cayman Chemical (Ann Arbor, MI, USA). Primers for RT-PCR were from Integrated DNA Technologies (Coralville, IA, USA). 5-BDBD, ADP (pre-treated with hexokinase as per [41]), ATP, BAPTA-AM, BzATP, hexokinase from *Saccharomyces cerevisiae*, ivermectin, MEM non-essential amino acid solution, paraformaldehyde, paroxetine, phosphate buffered saline (PBS), poly-D-lysine hydrobromide ( $5 \mu\text{g}\cdot\text{mL}^{-1}$  working stock), pluronic F-127, saponin, suramin and UTP were from Sigma-Aldrich (St. Louis, MO, USA). DMEM/F12 medium, ExoSAP-IT, Fura-2 AM, GlutaMAX, penicillin-streptomycin and 0.05% trypsin-EDTA were from ThermoFisher Scientific (Melbourne, Australia). 2MeSADP, AR-C118925, thapsigargin and TNP-ATP were from Tocris Bioscience (Bristol, UK).

### 4.2. Cells

DH82 cells were obtained from the European Collection of Authenticated Cell Cultures (ECACC cat. no. 94062922, RRID: CVCL\_2018). DH82 cells were cultured in DMEM/F12 medium supplemented with 10% FBS, 2 mM GlutaMAX, 100 U/mL penicillin, 100  $\mu\text{g}/\text{mL}$  streptomycin and 1% non-essential amino acids at 37 °C/5%  $\text{CO}_2$ . Cells were routinely found to be negative for mycoplasma contamination using the MycoAlert Mycoplasma Detection Kit (Lonza, Waverley, Australia).

### 4.3. RNA Isolation, cDNA Synthesis and RT-PCR

Total RNA was extracted from DH82 cells using the ISOLATE II RNA Mini Kit (Bioline, London, UK) according to manufacturer's instructions. cDNA was synthesised from RNA using the qScript cDNA SuperMix Kit (Quanta Biosciences, Gaithersburg, MD, USA) according to manufacturer's instructions. RT-PCR amplification of cDNA was carried out using the primer pairs and conditions listed in Table S1, the MangoTaq DNA polymerase kit (Bioline) and a Mastercycler Pro S (Eppendorf, Hamburg, Germany). PCR cycling consisted of initial denaturation at 95 °C for 2 min, followed by 35 cycles of denaturation at 95 °C for 30 s, annealing at 49–61 °C for 30 s and extension at 72 °C for 1 min. Amplicons were treated with ExoSAP-IT and loaded onto a 1% agarose gel and imaged using GelRed Nucleic Acid Gel Stain (Biotium, Fremont, CA, USA) and a Bio-Rad Molecular Imager Gel Doc XR+ (Hercules, CA, USA). Densitometry quantification was carried out using ImageJ [87] analysis software.

### 4.4. Measurement of Intracellular $\text{Ca}^{2+}$

Measurements of intracellular  $\text{Ca}^{2+}$  were determined using Fura-2 AM as previously described [41]. Recordings were performed in extracellular  $\text{Ca}^{2+}$  solution (ECS; 145 mM NaCl, 2 mM  $\text{CaCl}_2$ , 1 mM  $\text{MgCl}_2$ , 5 mM KCl, 13 mM glucose and 10 mM HEPES, pH 7.4) or in  $\text{Ca}^{2+}$  free solution (145 mM NaCl, 1 mM  $\text{MgCl}_2$ , 5 mM KCl, 13 mM glucose and 10 mM HEPES, pH 7.4) for recordings in absence of  $\text{Ca}^{2+}$ . Cells were plated at  $6 \times 10^4$  cells/well in poly-D-lysine-coated black-walled  $\mu\text{Clear}$  bottom 96-well plates (Greiner Bio-One, Frickenheisen, Germany) and incubated at 37 °C/5%  $\text{CO}_2$  for 18–24 h. Cells were washed in ECS then preincubated with Fura-2 AM loading buffer (2.5  $\mu\text{M}$  Fura-2 AM/0.2% pluronic acid in ECS) in the dark for 30 min at 37 °C. Prior to recording fluorescence, excess Fura-2 was removed and cells were washed with ECS (or  $\text{Ca}^{2+}$  free solution for recordings in absence of  $\text{Ca}^{2+}$ ), then incubated for a further 20 min to allow for complete de-esterification. Fura-2 fluorescence emission at 510 nm was recorded every 5 s at 37 °C using a Flexstation3 (Molecular Devices, Sunnyvale, CA, USA) following excitation at 340 and 380 nm. Recordings were taken for 15 s prior to addition of compounds to establish baseline fluorescence then for 3–5 min after addition of agonists. Where indicated, cells were preincubated with antagonists for up to 30 min prior to addition of nucleotides. The relative change in

intracellular  $\text{Ca}^{2+}$  ( $\Delta\text{Ca}^{2+}$ ) was calculated as ratio of Fura-2 fluorescence following excitation at 340 nm and 380 nm ( $F_{340/380}$ ) was determined and normalized to the mean basal fluorescence according to the formula (1):

$$\Delta\text{Ca}^{2+} = \frac{\Delta F}{F} = \frac{F - F_{\text{rest}}}{F_{\text{rest}}} \quad (1)$$

where  $F$  is the  $F_{340/380}$  at any given time and  $F_{\text{rest}}$  is the mean fluorescence of the given well prior to the addition of nucleotides [88]. To investigate endogenous P2X and P2Y receptor-mediated  $\text{Ca}^{2+}$  responses in DH82 canine macrophages, both the peak  $\text{Ca}^{2+}$  response ( $F_{340/380}$ ) and the net  $\text{Ca}^{2+}$  movement (calculated as area under the curve using GraphPad Prism) were calculated and, where indicated, used for fitting concentration-response curves fit to the Hill equation using the least squares method. Decay time ( $\tau$ , time constant) was calculated from the peak  $F_{340/380}$  using the nonlinear regression one phase decay model for GraphPad Prism. Decay times were not calculated where no response to agonists was recorded. Where antagonist  $\text{IC}_{50}$  was calculated against the approximate  $\text{EC}_{80}$  of ATP or UTP, responses were normalized to the response in absence of antagonist to allow data to be fit to a curve.

#### 4.5. Immunocytochemistry and Confocal Microscopy

Cells were plated at  $1 \times 10^5$  cells/18 mm glass coverslip in 24-well plates (Greiner Bio-One) and incubated at  $37^\circ\text{C}/5\% \text{CO}_2$  overnight prior to use. Cells were fixed with 3% (*w/v*) paraformaldehyde at  $4^\circ\text{C}$  for 15 min then washed three times with PBS. Cells were permeabilized with 0.1% (*w/v*) saponin resuspended in a blocking buffer (2% BSA (*w/v*) in PBS) at room temperature for 15 min and then incubated with anti-P2Y<sub>2</sub> (1:250; Alomone, cat no. APR-102, RRID: AB\_2756769) or anti-P2X<sub>4</sub> (1:250; Sigma-Aldrich cat no. SAB2500734, RRID:AB\_10604119) primary antibody in 2% BSA/PBS at room temperature for 2 h. Cells were washed three times with PBS and then incubated with Alexa Fluor594-conjugated anti-rabbit (1:200; Abcam cat no. ab150080, RRID: AB\_2650602), or Alexa Fluor594-conjugated anti-goat (1:200; Abcam cat no. ab150136, RRID: AB\_2782994) secondary antibody in 2% BSA/PBS at room temperature for 60 min. Cells were washed three times with PBS and then incubated with secondary antibody in 2% BSA/PBS at room temperature for 60 min. Washed coverslips were mounted onto a glass slide using 50% glycerol in PBS and sealed with nail polish. Cells were visualized on a Leica (Mannheim, Germany) SP5 confocal microscope.

#### 4.6. Data and Statistical Analysis

All data were analysed using GraphPad Prism 5. Half-maximal effective and inhibitory concentrations ( $\text{EC}_{50}$  and  $\text{IC}_{50}$ , respectively) are expressed as their negative logarithm ( $\text{pEC}_{50}/\text{pIC}_{50}$ )  $\pm$  SEM. Data were compared using a two-tailed Student's *t* test or one-way ANOVA with Bonferroni post hoc test for single or multiple comparisons, respectively. Multiple comparisons involving two interdependent variables were analysed using a two-way ANOVA with Bonferroni post hoc test. Throughout this study  $p < 0.05$  was considered statistically significant.

#### 4.7. Nomenclature of Targets and Ligands

All targets and ligands used throughout this manuscript conform with the guidelines outlined by the International Union of Basic and Clinical Pharmacology and British Pharmacological Society (IUPHAR/BPS) Guide to Pharmacology [40,89].

**Supplementary Materials:** Supplementary materials can be found at <http://www.mdpi.com/1422-0067/21/22/8572/s1>.

**Author Contributions:** Conceptualization: R.A.S., L.O., R.S.; methodology: R.A.S.; formal analysis: R.A.S.; investigation: R.A.S., N.A.M.; resources: L.O., R.S.; data curation: R.A.S.; writing—original draft preparation: R.A.S.; writing—review and editing: R.A.S., N.A.M., L.O., R.S.; visualization: R.A.S.; supervision: L.O., R.S.; project administration: R.S.; funding acquisition: R.S. All authors have read and agreed to the published version of the manuscript.



**Funding:** This research was funded by the American Kennel Club Canine Health Foundation, grant number 01985. R.A.S. was supported through an Australian Government Research Training Program Scholarship. L.O. is supported by a National Health and Medical Research Council (NHMRC) of Australia Boosting Dementia Research Leadership Fellowship (APP1135720). R.S. is supported by Molecular Horizons (University of Wollongong, Wollongong).

**Acknowledgments:** We thank the staff of the Technical Services Unit of the Illawarra Health and Medical Research Institute for technical assistance.

**Conflicts of Interest:** The authors declare no conflict of interest. The funders had no role in the design of the study; in the collection, analyses, or interpretation of data; in the writing of the manuscript; or in the decision to publish the results.

## Abbreviations

2-APB	2-Aminoethoxydiphenyl borate
2MeSADP	2-Methylthio-ADP
ADP	Adenosine 5'-diphosphate
ATP	Adenosine 5'-triphosphate
BAPTA-AM	1,2-Bis(2-aminophenoxy)ethane- <i>N,N,N',N'</i> -tetraacetic acid tetrakis(acetoxymethyl ester)
BzATP	3'-O-(4-Benzoyl)benzoyl-ATP
CNS	Central nervous system
CCL2	C-C chemokine ligand 2
CCR2	C-C chemokine receptor 2
DMSO	Dimethyl sulfoxide
EC <sub>50</sub>	Half maximal effective concentration
EGTA	Ethylene glycol tetraacetic acid
FBS	Fetal Bovine Serum
IC <sub>50</sub>	Half-maximal inhibitory concentration
IL	Interleukin
IP <sub>3</sub>	Inositol triphosphate
LPS	Lipopolysaccharide
MDCK	Madin Darby canine kidney
PLC	Phospholipase C
TNF	Tumor necrosis factor
TNP	2',3'-O-(2,4,6-Trinitrophenyl)
UDP	Uridine 5'-diphosphate
UTP	Uridine 5'-triphosphate

## References

- Ulmann, L.; Hatcher, J.P.; Hughes, J.P.; Chaumont, S.; Green, P.J.; Conquet, F.; Buell, G.N.; Reeve, A.J.; Chessell, I.P.; Rassendren, F. Up-Regulation of P2X4 Receptors in Spinal Microglia after Peripheral Nerve Injury Mediates BDNF Release and Neuropathic Pain. *J. Neurosci.* **2008**, *28*, 11263–11268. [[CrossRef](#)] [[PubMed](#)]
- Ulmann, L.; Hirbec, H.; Rassendren, F. P2X4 receptors mediate PGE<sub>2</sub> release by tissue-resident macrophages and initiate inflammatory pain. *EMBO J.* **2010**, *29*, 2290–2300. [[CrossRef](#)] [[PubMed](#)]
- Zhu, H.; Yu, Y.; Zheng, L.; Wang, L.; Li, C.; Yu, J.; Wei, J.; Wang, C.; Zhang, J.; Xu, S.; et al. Chronic inflammatory pain upregulates expression of P2Y2 receptor in small-diameter sensory neurons. *Metab. Brain Dis.* **2015**, *30*, 1349–1358. [[CrossRef](#)] [[PubMed](#)]
- Li, N.; Lu, Z.Y.; Yu, L.H.; Burnstock, G.; Deng, X.M.; Ma, B. Inhibition of G protein-coupled P2Y2 receptor induced analgesia in a rat model of trigeminal neuropathic pain. *Mol. Pain* **2014**, *10*, 21. [[CrossRef](#)]
- Su, W.F.; Wu, F.; Jin, Z.H.; Gu, Y.; Chen, Y.T.; Fei, Y.; Chen, H.; Wang, Y.X.; Xing, L.Y.; Zhao, Y.Y.; et al. Overexpression of P2X4 receptor in Schwann cells promotes motor and sensory functional recovery and remyelination via BDNF secretion after nerve injury. *Glia* **2019**, *67*, 78–90. [[CrossRef](#)]
- Zabala, A.; Vazquez-Villoldo, N.; Rissiek, B.; Gejo, J.; Martin, A.; Palomino, A.; Perez-Samartín, A.; Pulagam, K.R.; Lukowiak, M.; Capetillo-Zarate, E.; et al. P2X4 receptor controls microglia activation and favors remyelination in autoimmune encephalitis. *EMBO Mol. Med.* **2018**, *10*, e8743. [[CrossRef](#)]

7. Burnstock, G. Pathophysiology and therapeutic potential of purinergic signaling. *Pharmacol. Rev.* **2006**, *58*, 58–86. [[CrossRef](#)]
8. Stokes, L.; Surprenant, A. Purinergic P2Y<sub>2</sub> receptors induce increased MCP-1/CCL2 synthesis and release from rat alveolar and peritoneal macrophages. *J. Immunol.* **2007**, *179*, 6016–6023. [[CrossRef](#)]
9. Layhadi, J.A.; Fountain, S.J. ATP-Evoked Intracellular Ca<sup>2+</sup> Responses in M-CSF Differentiated Human Monocyte-Derived Macrophage are Mediated by P2X<sub>4</sub> and P2Y<sub>11</sub> Receptor Activation. *Int. J. Mol. Sci.* **2019**, *20*, 5113. [[CrossRef](#)]
10. Higgins, K.R.; Kovacevic, W.; Stokes, L. Nucleotides regulate secretion of the inflammatory chemokine CCL2 from human macrophages and monocytes. *Mediators Inflamm.* **2014**, *2014*. [[CrossRef](#)]
11. Layhadi, J.A.; Turner, J.; Crossman, D.; Fountain, S.J. ATP Evokes Ca<sup>2+</sup> Responses and CXCL5 Secretion via P2X<sub>4</sub> Receptor Activation in Human Monocyte-Derived Macrophages. *J. Immunol.* **2018**, *200*, 1159–1168. [[CrossRef](#)] [[PubMed](#)]
12. Bowler, J.W.; Bailey, R.J.; North, R.A.; Surprenant, A. P2X<sub>4</sub>, P2Y<sub>1</sub> and P2Y<sub>2</sub> receptors on rat alveolar macrophages. *Br. J. Pharmacol.* **2003**, *140*, 567–575. [[CrossRef](#)] [[PubMed](#)]
13. Stokes, L.; Surprenant, A. Dynamic regulation of the P2X<sub>4</sub> receptor in alveolar macrophages by phagocytosis and classical activation. *Eur. J. Immunol.* **2009**, *39*, 986–995. [[CrossRef](#)] [[PubMed](#)]
14. Vargas-Martínez, E.M.; Gómez-Coronado, K.S.; Espinosa-Luna, R.; Valdez-Morales, E.E.; Barrios-García, T.; Barajas-Espinosa, A.; Ochoa-Cortes, F.; Montaña, L.M.; Barajas-López, C.; Guerrero-Alba, R. Functional expression of P2X<sub>1</sub>, P2X<sub>4</sub> and P2X<sub>7</sub> purinergic receptors in human monocyte-derived macrophages. *Eur. J. Pharmacol.* **2020**, *888*, 173460. [[CrossRef](#)] [[PubMed](#)]
15. Chessell, I.P.; Hatcher, J.P.; Bountra, C.; Michel, A.D.; Hughes, J.P.; Green, P.; Egerton, J.; Murfin, M.; Richardson, J.; Peck, W.L.; et al. Disruption of the P2X<sub>7</sub> purinoceptor gene abolishes chronic inflammatory and neuropathic pain. *Pain* **2005**, *114*, 386–396. [[CrossRef](#)] [[PubMed](#)]
16. Tsuda, M.; Kuboyama, K.; Inoue, T.; Nagata, K.; Tozaki-Saitoh, H.; Inoue, K. Behavioral phenotypes of mice lacking purinergic P2X<sub>4</sub> receptors in acute and chronic pain assays. *Mol. Pain* **2009**, *5*, 28. [[CrossRef](#)]
17. Trang, T.; Beggs, S.; Wan, X.; Salter, M.W. P2X<sub>4</sub>-receptor-mediated synthesis and release of brain-derived neurotrophic factor in microglia is dependent on calcium and p38-mitogen-activated protein kinase activation. *J. Neurosci.* **2009**, *29*. [[CrossRef](#)] [[PubMed](#)]
18. Tsuda, M.; Shigemoto-Mogami, Y.; Koizumi, S.; Mizokoshi, A.; Kohsaka, S.; Salter, M.W.; Inoue, K. P2X<sub>4</sub> receptors induced in spinal microglia gate tactile allodynia after nerve injury. *Nature* **2003**, *424*. [[CrossRef](#)]
19. Wellman, M.L.; Krakowka, S.; Jacobs, R.M.; Kociba, G.J. A macrophage-monocyte cell line from a dog with malignant histiocytosis. *In Vitro Cell. Dev. Biol.* **1988**, *24*, 223–229. [[CrossRef](#)]
20. Herrmann, I.; Gotovina, J.; Fazekas-Singer, J.; Fischer, M.B.; Hufnagl, K.; Bianchini, R.; Jensen-Jarolim, E. Canine macrophages can like human macrophages be in vitro activated toward the M2a subtype relevant in allergy. *Dev. Comp. Immunol.* **2018**, *82*, 118–127. [[CrossRef](#)]
21. Heinrich, F.; Contioso, V.B.; Stein, V.M.; Carlson, R.; Tipold, A.; Ulrich, R.; Puff, C.; Baumgärtner, W.; Spitzbarth, I. Passage-dependent morphological and phenotypical changes of a canine histiocytic sarcoma cell line (DH82 cells). *Vet. Immunol. Immunopathol.* **2015**, *163*, 86–92. [[CrossRef](#)] [[PubMed](#)]
22. Barnes, A.; Bee, A.; Bell, S.; Gilmore, W.; Mee, A.; Morris, R.; Carter, S.D. Immunological and inflammatory characterisation of three canine cell lines: K1, K6 and DH82. *Vet. Immunol Immunopathol.* **2000**, *75*, 9–25. [[CrossRef](#)]
23. Mendonça, P.H.B.; da Rocha, R.F.D.B.; Moraes, J.B.d.B.; LaRocque-de-Freitas, I.F.; Logullo, J.; Morrot, A.; Nunes, M.P.; Freire-de-Lima, C.G.; Decote-Ricardo, D. Canine Macrophage DH82 Cell Line As a Model to Study Susceptibility to Trypanosoma cruzi Infection. *Front. Immunol.* **2017**, *8*, 604. [[CrossRef](#)] [[PubMed](#)]
24. Armando, F.; Gambini, M.; Corradi, A.; Giudice, C.; Pfankuche, V.M.; Brogden, G.; Attig, F.; von Kockritz-Blickwede, M.; Baumgartner, W.; Puff, C. Oxidative Stress in Canine Histiocytic Sarcoma Cells Induced by an Infection with Canine Distemper Virus Led to a Dysregulation of HIF-1alpha Downstream Pathway Resulting in a Reduced Expression of VEGF-B in vitro. *Viruses* **2020**, *12*, 200. [[CrossRef](#)]
25. Nadaes, N.R.; Silva da Costa, L.; Santana, R.C.; LaRocque-de-Freitas, I.F.; Vivarini, Á.C.; Soares, D.C.; Wardini, A.B.; Gazos Lopes, U.; Saraiva, E.M.; Freire-de-Lima, C.G.; et al. DH82 Canine and RAW264.7 Murine Macrophage Cell Lines Display Distinct Activation Profiles Upon Interaction with Leishmania infantum and Leishmania amazonensis. *Front. Cell Infect. Microbiol.* **2020**, *10*, 247. [[CrossRef](#)]

26. Fujimoto, Y.; Nakatani, N.; Kubo, T.; Semi, Y.; Yoshida, N.; Nakajima, H.; Iseri, T.; Azuma, Y.T.; Takeuchi, T. Adenosine and ATP affect LPS-induced cytokine production in canine macrophage cell line DH82 cells. *J. Vet. Med. Sci.* **2012**, *74*, 27–34. [[CrossRef](#)]
27. Zheng, X.; Zhu, Y.; Zhao, Z.; Yan, L.; Xu, T.; Wang, X.; He, H.; Xia, X.; Zheng, W.; Xue, X. RNA sequencing analyses of gene expressions in a canine macrophages cell line DH82 infected with canine distemper virus. *Infect. Genet. Evol.* **2020**, *80*, 104206. [[CrossRef](#)]
28. Sluyter, R. The P2X7 Receptor. *Adv. Exp. Med. Biol.* **2017**, *1051*, 17–53.
29. Stevenson, R.O.; Taylor, R.M.; Wiley, J.S.; Sluyter, R. The P2X7 receptor mediates the uptake of organic cations in canine erythrocytes and mononuclear leukocytes: Comparison to equivalent human cell types. *Purinergic Signal.* **2009**, *5*, 385–394. [[CrossRef](#)]
30. Jalilian, I.; Peranec, M.; Curtis, B.L.; Seavers, A.; Spildrejorde, M.; Sluyter, V.; Sluyter, R. Activation of the damage-associated molecular pattern receptor P2X7 induces interleukin-1 beta release from canine monocytes. *Vet. Immunol. Immunopathol.* **2012**, *149*, 86–91. [[CrossRef](#)]
31. Ase, A.R.; Honson, N.S.; Zaghdane, H.; Pfeifer, T.A.; Seguela, P. Identification and characterization of a selective allosteric antagonist of human P2X4 receptor channels. *Mol. Pharmacol.* **2015**, *87*, 606–616. [[CrossRef](#)] [[PubMed](#)]
32. Honore, P.; Donnelly-Roberts, D.; Namovic, M.; Zhong, C.M.; Wade, C.; Chandran, P.; Zhu, C.; Carroll, W.; Perez-Medrano, A.; Iwakura, Y.; et al. The antihyperalgesic activity of a selective P2X7 receptor antagonist, A-839977, is lost in IL-1 alpha beta knockout mice. *Behav. Brain Res.* **2009**, *204*, 77–81. [[CrossRef](#)] [[PubMed](#)]
33. Humphreys, B.D.; Virginio, C.; Surprenant, A.; Rice, J.; Dubyak, G.R. Isoquinolines as antagonists of the P2X7 nucleotide receptor: High selectivity for the human versus rat receptor homologues. *Mol. Pharmacol.* **1998**, *54*, 22–32. [[CrossRef](#)] [[PubMed](#)]
34. Layhadi, J.A.; Fountain, S.J. P2X4 Receptor-Dependent Ca<sup>2+</sup> Influx in Model Human Monocytes and Macrophages. *Int. J. Mol. Sci.* **2017**, *18*, 2261. [[CrossRef](#)] [[PubMed](#)]
35. Micklewright, J.J.; Layhadi, J.A.; Fountain, S.J. P2Y<sub>12</sub> receptor modulation of ADP-evoked intracellular Ca<sup>2+</sup> signalling in THP-1 human monocytic cells. *Br. J. Pharmacol.* **2018**, *175*, 2483–2491. [[CrossRef](#)] [[PubMed](#)]
36. Zhang, Z.; Hao, K.; Li, H.; Lu, R.; Liu, C.; Zhou, M.; Li, B.; Meng, Z.; Hu, Q.; Jiang, C. Design, synthesis and anti-inflammatory evaluation of 3-amide benzoic acid derivatives as novel P2Y<sub>14</sub> receptor antagonists. *Eur. J. Med. Chem.* **2019**, *181*, 111564. [[CrossRef](#)]
37. Tu, Y.M.; Gong, C.X.; Ding, L.; Liu, X.Z.; Li, T.; Hu, F.F.; Wang, S.; Xiong, C.P.; Liang, S.D.; Xu, H. A high concentration of fatty acids induces TNF-alpha as well as NO release mediated by the P2X4 receptor, and the protective effects of puerarin in RAW264.7 cells. *Food Funct.* **2017**, *8*, 4336–4346. [[CrossRef](#)]
38. Gadeock, S.; Tran, J.; Georgiou, J.G.; Jalilian, I.; Taylor, R.M.; Wiley, J.S.; Sluyter, R. TGF-beta 1 prevents up-regulation of the P2X7 receptor by IFN-gamma and LPS in leukemic THP-1 monocytes. *Biochim. Biophys. Acta* **2010**, *1798*, 2058–2066. [[CrossRef](#)]
39. Jacobson, K.A.; Delicado, E.G.; Gachet, C.; Kennedy, C.; von Kügelgen, I.; Li, B.; Miras-Portugal, M.T.; Novak, I.; Schöneberg, T.; Perez-Sen, R.; et al. Update of P2Y Receptor Pharmacology: IUPHAR Review:27. *Br. J. Pharmacol.* **2020**, *177*, 2413–2433. [[CrossRef](#)]
40. Alexander, S.P.H.; Mathie, A.; Peters, J.A.; Veale, E.L.; Striessnig, J.; Kelly, E.; Armstrong, J.F.; Faccenda, E.; Harding, S.D.; Pawson, A.J.; et al. The Concise Guide to Pharmacology 2019/20: Ion channels. *Br. J. Pharmacol.* **2019**, *176* (Suppl. 1), S142–S228. [[CrossRef](#)]
41. Sophocleous, R.A.; Berg, T.; Finol-Urdaneta, R.K.; Sluyter, V.; Keshiya, S.; Bell, L.; Curtis, S.J.; Curtis, B.L.; Seavers, A.; Bartlett, R.; et al. Pharmacological and genetic characterisation of the canine P2X4 receptor. *Br. J. Pharmacol.* **2020**, *177*, 2812–2829. [[CrossRef](#)] [[PubMed](#)]
42. Virginio, C.; Robertson, G.; Surprenant, A.; North, R.A. Trinitrophenyl-Substituted Nucleotides Are Potent Antagonists Selective for P2X1, P2X3, and Heteromeric P2X2/3 Receptors. *Mol. Pharmacol.* **1998**, *53*, 969. [[PubMed](#)]
43. Nagata, K.; Imai, T.; Yamashita, T.; Tsuda, M.; Tozaki-Saitoh, H.; Inoue, K. Antidepressants inhibit P2X4 Receptor function: A possible involvement in neuropathic pain relief. *Mol. Pain* **2009**, *5*, 20. [[CrossRef](#)]
44. Abdelrahman, A.; Namasivayam, V.; Hinz, S.; Schiedel, A.C.; Kose, M.; Burton, M.; El-Tayeb, A.; Gillard, M.; Bajorath, J.; de Ryck, M.; et al. Characterization of P2X4 receptor agonists and antagonists by calcium influx and radioligand binding studies. *Biochem. Pharmacol.* **2017**, *125*, 41–54. [[CrossRef](#)] [[PubMed](#)]

45. Wang, W.; Xiang, Z.-H.; Jiang, C.-L.; Liu, W.-Z.; Shang, Z.-L. Effects of antidepressants on P2X7 receptors. *Psychiatry Res.* **2016**, *242*, 281–287. [[CrossRef](#)]
46. Dao-Ung, P.; Skarratt, K.K.; Fuller, S.J.; Stokes, L. Paroxetine suppresses recombinant human P2X7 responses. *Purinergic Signal.* **2015**, *11*, 481–490. [[CrossRef](#)]
47. Abbracchio, M.P.; Burnstock, G.; Boeynaems, J.M.; Barnard, E.A.; Boyer, J.L.; Kennedy, C.; Knight, G.E.; Fumagalli, M.; Gachet, C.; Jacobson, K.A.; et al. International Union of Pharmacology LVIII: Update on the P2Y G protein-coupled nucleotide receptors: From molecular mechanisms and pathophysiology to therapy. *Pharmacol. Rev.* **2006**, *58*, 281–341. [[CrossRef](#)]
48. Thastrup, O.; Cullen, P.J.; Drøbak, B.K.; Hanley, M.R.; Dawson, A.P. Thapsigargin, a tumor promoter, discharges intracellular  $\text{Ca}^{2+}$  stores by specific inhibition of the endoplasmic reticulum  $\text{Ca}^{2+}$ -ATPase. *Proc. Natl. Acad. Sci. USA* **1990**, *87*, 2466–2470. [[CrossRef](#)]
49. Zamboni, A.C.; Hughes, R.J.; Meszaros, J.G.; Wu, J.J.; Torres, B.; Brunton, L.L.; Insel, P.A. P2Y<sub>2</sub> receptor of MDCK cells: Cloning, expression, and cell-specific signaling. *Am. J. Physiol. Renal Physiol.* **2000**, *279*, F1045–F1052. [[CrossRef](#)]
50. Kempson, S.A.; Edwards, J.M.; Osborn, A.; Sturek, M. Acute inhibition of the betaine transporter by ATP and adenosine in renal MDCK cells. *Am. J. Physiol. Renal Physiol.* **2008**, *295*, F108–F117. [[CrossRef](#)]
51. Charlton, S.J.; Brown, C.A.; Weisman, G.A.; Turner, J.T.; Erb, L.; Boarder, M.R. Cloned and transfected P2Y<sub>4</sub> receptors: Characterization of a suramin and PPADS-insensitive response to UTP. *Br. J. Pharmacol.* **1996**, *119*, 1301–1303. [[CrossRef](#)] [[PubMed](#)]
52. Rafahi, M.; Burbiel, J.C.; Attah, I.Y.; Abdelrahman, A.; Müller, C.E. Synthesis, characterization, and in vitro evaluation of the selective P2Y<sub>2</sub> receptor antagonist AR-C118925. *Purinergic Signal.* **2017**, *13*, 89–103. [[CrossRef](#)] [[PubMed](#)]
53. Wolff, S.C.; Qi, A.D.; Harden, T.K.; Nicholas, R.A. Polarized expression of human P2Y receptors in epithelial cells from kidney, lung, and colon. *Am. J. Physiol. Cell Physiol.* **2005**, *288*, C624–C632. [[CrossRef](#)] [[PubMed](#)]
54. Qi, A.D.; Wolff, S.C.; Nicholas, R.A. The apical targeting signal of the P2Y<sub>2</sub> receptor is located in its first extracellular loop. *J. Biol. Chem.* **2005**, *280*, 29169–29175. [[CrossRef](#)]
55. Xue, X.; Zhu, Y.; Yan, L.; Wong, G.; Sun, P.; Zheng, X.; Xia, X. Antiviral efficacy of favipiravir against canine distemper virus infection in vitro. *BMC Vet. Res.* **2019**, *15*, 316. [[CrossRef](#)]
56. Pfankuche, V.M.; Sayed-Ahmed, M.; Contioso, V.B.; Spitzbarth, I.; Rohn, K.; Ulrich, R.; Deschl, U.; Kalkuhl, A.; Baumgärtner, W.; Puff, C. Persistent Morbillivirus Infection Leads to Altered Cortactin Distribution in Histiocytic Sarcoma Cells with Decreased Cellular Migration Capacity. *PLoS ONE* **2016**, *11*, e0167517. [[CrossRef](#)]
57. Armando, F.; Gambini, M.; Corradi, A.; Becker, K.; Marek, K.; Pfankuche, V.M.; Mergani, A.E.; Brogden, G.; de Buhr, N.; von Köckritz-Blickwede, M.; et al. Mesenchymal to epithelial transition driven by canine distemper virus infection of canine histiocytic sarcoma cells contributes to a reduced cell motility in vitro. *J. Cell Mol. Med.* **2020**, *24*, 9332–9348. [[CrossRef](#)]
58. Balazs, B.; Danko, T.; Kovacs, G.; Koles, L.; Hediger, M.A.; Zsembery, A. Investigation of the inhibitory effects of the benzodiazepine derivative, 5-BDBD on P2X4 purinergic receptors by two complementary methods. *Cell Physiol. Biochem.* **2013**, *32*, 11–24. [[CrossRef](#)]
59. Stokes, L.; Bidula, S.; Bibič, L.; Allum, E. To Inhibit or Enhance? Is There a Benefit to Positive Allosteric Modulation of P2X Receptors? *Front. Pharmacol.* **2020**, *11*, 627. [[CrossRef](#)]
60. von Kugelgen, I. Pharmacology of P2Y receptors. *Brain Res. Bull.* **2019**. [[CrossRef](#)]
61. Jan, C.R.; Ho, C.M.; Wu, S.N.; Tseng, C.J. Mechanisms of rise and decay of ADP-evoked calcium signal in MDCK cells. *Chin. J. Physiol.* **1998**, *41*, 67–73. [[PubMed](#)]
62. Katzur, A.C.; Koshimizu, T.-A.; Tomic, M.; Schultze-Mosgau, A.; Ortmann, O.; Stojilkovic, S.S. Expression and Responsiveness of P2Y<sub>2</sub> Receptors in Human Endometrial Cancer Cell Lines. *J. Clin. Endocrinol. Metab.* **1999**, *84*, 4085–4091. [[CrossRef](#)] [[PubMed](#)]
63. Wildman, S.S.; Unwin, R.J.; King, B.F. Extended pharmacological profiles of rat P2Y<sub>2</sub> and rat P2Y<sub>4</sub> receptors and their sensitivity to extracellular  $\text{H}^{+}$  and  $\text{Zn}^{2+}$  ions. *Br. J. Pharmacol.* **2003**, *140*, 1177–1186. [[CrossRef](#)] [[PubMed](#)]
64. Maier, T.; Güell, M.; Serrano, L. Correlation of mRNA and protein in complex biological samples. *FEBS Lett.* **2009**, *583*, 3966–3973. [[CrossRef](#)] [[PubMed](#)]

65. Post, S.R.; Rump, L.C.; Zambon, A.; Hughes, R.J.; Buda, M.D.; Jacobson, J.P.; Kao, C.C.; Insel, P.A. ATP activates cAMP production via multiple purinergic receptors in MDCK-D1 epithelial cells. Blockade of an autocrine/paracrine pathway to define receptor preference of an agonist. *J. Biol. Chem.* **1998**, *273*, 23093–23097. [[CrossRef](#)] [[PubMed](#)]
66. Qi, A.D.; Zambon, A.C.; Insel, P.A.; Nicholas, R.A. An arginine/glutamine difference at the juxtaposition of transmembrane domain 6 and the third extracellular loop contributes to the markedly different nucleotide selectivities of human and canine P2Y<sub>11</sub> receptors. *Mol. Pharmacol.* **2001**, *60*, 1375–1382. [[CrossRef](#)]
67. Communi, D.; Robaye, B.; Boeynaems, J.M. Pharmacological characterization of the human P2Y<sub>11</sub> receptor. *Br. J. Pharmacol.* **1999**, *128*, 1199–1206. [[CrossRef](#)]
68. Hughes, R.J.; Torres, B.; Zambon, A.; Arthur, D.; Bohmann, C.; Rump, L.C.; Insel, P.A. Expression of multiple P2Y receptors by MDCK-D1 cells: P2Y<sub>1</sub> receptor cloning and signaling. *Drug Dev. Res.* **2003**, *59*, 1–7. [[CrossRef](#)]
69. Nicholas, R.A.; Watt, W.C.; Lazarowski, E.R.; Li, Q.; Harden, K. Uridine nucleotide selectivity of three phospholipase C-activating P2 receptors: Identification of a UDP-selective, a UTP-selective, and an ATP- and UTP-specific receptor. *Mol. Pharmacol.* **1996**, *50*, 224–229.
70. Communi, D.; Parmentier, M.; Boeynaems, J.M. Cloning, functional expression and tissue distribution of the human P2Y<sub>6</sub> receptor. *Biochem. Biophys. Res. Commun.* **1996**, *222*, 303–308. [[CrossRef](#)]
71. Insel, P.A.; Ostrom, R.S.; Zambon, A.C.; Hughes, R.J.; Balboa, M.A.; Shehnaz, D.; Gregorian, C.; Torres, B.; Firestein, B.L.; Xing, M.; et al. P2Y receptors of MDCK cells: Epithelial cell regulation by extracellular nucleotides. *Clin. Exp. Pharmacol. Physiol.* **2001**, *28*, 351–354. [[CrossRef](#)] [[PubMed](#)]
72. Liu, B.; Cao, W.; Li, J.; Liu, J. Lysosomal exocytosis of ATP is coupled to P2Y<sub>2</sub> receptor in marginal cells in the stria vascularis in neonatal rats. *Cell Calcium* **2018**, *76*, 62–71. [[CrossRef](#)] [[PubMed](#)]
73. Jones, C.A.; Chessell, I.P.; Simon, J.; Barnard, E.A.; Miller, K.J.; Michel, A.D.; Humphrey, P.P.A. Functional characterization of the P2X<sub>4</sub> receptor orthologues. *Br. J. Pharmacol.* **2000**, *129*, 388–394. [[CrossRef](#)] [[PubMed](#)]
74. Muzzachi, S.; Blasi, A.; Ciani, E.; Favia, M.; Cardone, R.A.; Marzulli, D.; Reshkin, S.J.; Merizzi, G.; Casavola, V.; Soleti, A.; et al. MED1101: A new dialdehydic compound regulating P2x7 receptor cell surface expression in U937 cells. *Biol. Cell* **2013**, *105*, 399–413. [[CrossRef](#)] [[PubMed](#)]
75. Bernier, L.P.; Ase, A.R.; Seguela, P. P2X receptor channels in chronic pain pathways. *Br. J. Pharmacol.* **2018**, *175*, 2219–2230. [[CrossRef](#)] [[PubMed](#)]
76. Inoue, K. Role of the P2X<sub>4</sub> receptor in neuropathic pain. *Curr. Opin. Pharmacol.* **2019**, *47*, 33–39. [[CrossRef](#)]
77. Domercq, M.; Matute, C. Targeting P2X<sub>4</sub> and P2X<sub>7</sub> receptors in multiple sclerosis. *Curr. Opin. Pharmacol.* **2019**, *47*, 119–125. [[CrossRef](#)]
78. Qureshi, O.S.; Paramasivam, A.; Yu, J.C.; Murrell-Lagnado, R.D. Regulation of P2X<sub>4</sub> receptors by lysosomal targeting, glycan protection and exocytosis. *J. Cell Sci.* **2007**, *120*, 3838–3849. [[CrossRef](#)]
79. Sivaramakrishnan, V.; Bidula, S.; Campwala, H.; Katikaneni, D.; Fountain, S.J. Constitutive lysosome exocytosis releases ATP and engages P2Y receptors in human monocytes. *J. Cell Sci.* **2012**, *125*, 4567–4575. [[CrossRef](#)]
80. Toyomitsu, E.; Tsuda, M.; Yamashita, T.; Tozaki-Saitoh, H.; Tanaka, Y.; Inoue, K. CCL2 promotes P2X<sub>4</sub> receptor trafficking to the cell surface of microglia. *Purinergic Signal.* **2012**, *8*, 301–310. [[CrossRef](#)]
81. Greenhalgh, A.D.; Zarruk, J.G.; Healy, L.M.; Baskar Jesudasan, S.J.; Jhelum, P.; Salmon, C.K.; Formanek, A.; Russo, M.V.; Antel, J.P.; McGavern, D.B.; et al. Peripherally derived macrophages modulate microglial function to reduce inflammation after CNS injury. *PLoS Biol.* **2018**, *16*, e2005264. [[CrossRef](#)] [[PubMed](#)]
82. Jagannathan, V.; Drogemuller, C.; Leeb, T. A comprehensive biomedical variant catalogue based on whole genome sequences of 582 dogs and eight wolves. *Anim. Genet.* **2019**, *50*, 695–704. [[CrossRef](#)] [[PubMed](#)]
83. Büscher, R.; Hoerning, A.; Patel, H.H.; Zhang, S.; Arthur, D.B.; Grasemann, H.; Ratjen, F.; Insel, P.A. P2Y<sub>2</sub> receptor polymorphisms and haplotypes in cystic fibrosis and their impact on Ca<sup>2+</sup> influx. *Pharmacogenet. Genom.* **2006**, *16*, 199–205. [[CrossRef](#)]
84. Stokes, L.; Scurrah, K.; Ellis, J.A.; Cromer, B.A.; Skarratt, K.K.; Gu, B.J.; Harrap, S.B.; Wiley, J.S. A loss-of-function polymorphism in the human P2X<sub>4</sub> receptor is associated with increased pulse pressure. *Hypertension* **2011**, *58*, 1086–1092. [[CrossRef](#)]
85. Sophocleous, R.A.; Sluyter, V.; Curtis, B.L.; Curtis, S.J.; Jurak, L.M.; Faulks, M.; Spildrejorde, M.; Gates, S.; Proctor, E.J.; Seavers, A.; et al. Association of a P2RX<sub>7</sub> gene missense variant with brachycephalic dog breeds. *Anim. Genet.* **2020**, *51*, 127–131. [[CrossRef](#)]

86. Spildrejorde, M.; Bartlett, R.; Stokes, L.; Jalilian, I.; Peranec, M.; Sluyter, V.; Curtis, B.L.; Skarratt, K.K.; Skora, A.; Bakhsh, T.; et al. R270C polymorphism leads to loss of function of the canine P2X7 receptor. *Physiol. Genom.* **2014**, *46*, 512–522. [[CrossRef](#)]
87. Rueden, C.T.; Schindelin, J.; Hiner, M.C.; DeZonia, B.E.; Walter, A.E.; Arena, E.T.; Eliceiri, K.W. ImageJ2: ImageJ for the next generation of scientific image data. *BMC Bioinform.* **2017**, *18*, 529. [[CrossRef](#)]
88. Paredes, R.M.; Etzler, J.C.; Watts, L.T.; Lechleiter, J.D. Chemical Calcium Indicators. *Methods (San Diego, Calif.)* **2008**, *46*, 143–151. [[CrossRef](#)]
89. Alexander, S.P.H.; Christopoulos, A.; Davenport, A.P.; Kelly, E.; Mathie, A.; Peters, J.A.; Veale, E.L.; Armstrong, J.F.; Faccenda, E.; Harding, S.D.; et al. The Concise Guide to Pharmacology 2019/20: G protein-coupled receptors. *Br. J. Pharmacol.* **2019**, *176*, S21–S141. [[CrossRef](#)]

**Publisher's Note:** MDPI stays neutral with regard to jurisdictional claims in published maps and institutional affiliations.



© 2020 by the authors. Licensee MDPI, Basel, Switzerland. This article is an open access article distributed under the terms and conditions of the Creative Commons Attribution (CC BY) license (<http://creativecommons.org/licenses/by/4.0/>).